Mon. Not. R. astr. Soc. (1978) **182**, 273–274 and *Microfiche* MN 182/1

The 5C 6 and 5C 7 surveys of radio sources

T. J. Pearson *Mullard Radio Astronomy Observatory, Cavendish Laboratory, Madingley Road, Cambridge CB3 0HE*

A. J. Kus *Universytet M. Kopernika, Instytut Astronomii, ul Chopina 12/18, 87-100 Toruń, Poland*

Received 1977 September 2

Extended summary. 5C 6 and 5C 7 continue the series of deep surveys made at 408 and 1407 MHz with the One-Mile telescope at Cambridge. They were intended (1) to provide a sample of faint radio sources suitable for further study; (2) to improve the statistics of source counts $N(S)$ and spectral-index distributions at low flux densities; (3) to study the isotropy of the distribution of faint sources. Each observed field is about 4° in diameter at 408 MHz and 1° in diameter at 1407 MHz, and the field-centres are $\alpha = 02^h\,14^m$, $\delta = 32°$ (5C 6) and $\alpha = 08^h\,17^m$, $\delta = 27°$ (5C 7). The synthesized beamwidths (FWHM) are 80 arcsec (408 MHz) and 23 arcsec (1407 MHz). The techniques of observation and data-analysis followed closely those used for 5C 5 (Pearson, T. J., 1975. *Mon. Not. R. astr. Soc.*, **171**, 475), with some minor variations which are noted in Section 2.

The sources detected in the two surveys are listed in Tables 2 and 3, which include 535 sources stronger than 10 mJy at 408 MHz and 121 stronger than 1.5 mJy at 1407 MHz. Right ascensions and declinations are given with an uncertainty varying between about 0.5 and 10 arcsec rms, depending on the intensity and the frequency of observation. Tables 2 and 3 also include descriptions of optical objects visible on the Palomar Sky Survey within about 20 arcsec of the radio sources.

The results were compared with independent observations of some of the stronger sources (Sections 4 and 5); there is no evidence for any error in the flux-density scales or the envelope-correction, systematic positional errors are less than 4 arcsec at the centres of the fields and any distortions of the coordinate systems are less than 0.03 per cent. (An error in the analysis of the earlier 5C surveys, causing a rotation of the coordinate system about the field centre, has been corrected.)

The 408-MHz source counts are presented in Table 9 and Fig. 6. 5C 6 and 5C 7 have generally higher source-densities than the earlier surveys 5C 2 and 5C 5, but the differences between the four surveys are not statistically signifi-

cant. The combined count from 5C 5, 6 and 7 (presented in differential form in Fig. 7 and in integral form in Fig. 8) defines the 'convergence' of the source count closely, and is in good agreement with the 408-MHz Molonglo and 610-MHz Westerbork counts. The statistical uncertainty in the 1407-MHz source counts is large, but there is no evidence for any variations between the 5C surveys; the combined count from 5C 5, 6 and 7, however, is significantly lower than that derived by Katgert from the third Westerbork survey (Fig. 9).

The spectral-index distributions of sources selected at 1407 MHz from 5C 5, 6 and 7 are all similar, with median $\alpha(408, 1407) = 0.80 \pm 0.03$. The form of the spectral-index distribution is similar to those of distributions from samples selected at higher flux densities.

There is no evidence that the sources detected in the three surveys are not distributed randomly and uniformly on the sky.

The full text of this paper may be found on *Microfiche* MN 182/1 distributed with this issue of *Monthly Notices*.

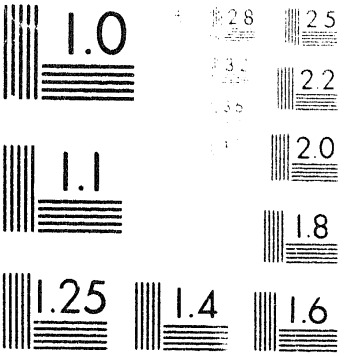

Monthly Notices
of the
ROYAL ASTRONOMICAL SOCIETY

VOL. 182, NO. 1, 1978

The 5C6 and 5C7 surveys of radio sources

T. J. Pearson and A. J. Kus

Published for the Royal Astronomical Society

Blackwell Scientific Publications

Oxford Microform Publications

The microfiches are 105 x 148mm archivally permanent silver halide film produced to internationally accepted standards in the NMA 98-image format

Microfiches produced by O.M.P., Blue Boar St., Oxford OX1 4EY and Micromedia, Bicester, Oxon

The 5C6 and 5C7 surveys of radio sources

T.J. Pearson *Mullard Radio Astronomy Observatory, Cavendish Laboratory, Madingley Road, Cambridge CB3 0HE, England*
A.J. Kus *Uniwersytet M. Kopernika, Instytut Astronomii, ul. Chopina 12/18, 87-100 Toruń, Poland*

Received 1977 June 20

Summary. 5C6 and 5C7 are aperture-synthesis surveys made with the Cambridge One-Mile telescope centred at $\alpha = 02^h\ 14^m$, $\delta = 32^o\ 00'$ and $\alpha = 08^h\ 17^m$, $\delta = 27^o\ 00'$, directions chosen to advance the study of the isotropy of faint sources. The positions and flux densities of 535 sources stronger than 10 mJy at 408 MHz and 121 stronger than 1.5 mJy at 1407 MHz are presented, with source counts and spectral-index distributions. The two source counts at 408 MHz are in good agreement with each other, although the source density is slightly higher than in 5C2 and 5C5. At 1407 MHz the source counts agree (within their uncertainty) with each other and with 5C5; the 5C counts agree with the Westerbork 1 survey but are lower than the corrected Westerbork 3 counts. The spectral index distributions of sources selected at 1407 MHz from 5C5, 5C6 and 5C7 are all similar, with median $\alpha(408,1407) = 0.80 \pm 0.03$.

1 Introduction

As part of a continuing study of the distribution of faint radio sources, two more deep surveys have been made with the One-Mile telescope at Cambridge. These surveys, 5C6 and 5C7, like the earlier surveys 5C2 (Pooley & Kenderdine 1968) and 5C5 (Pearson 1975) with which they are to be compared, are of regions of sky selected to be free of strong (i.e. 4C) sources. Each observed field is about 4^o in diameter at 408 MHz and 1^o in diameter at 1407 MHz. One motivation of the surveys was to study the isotropy of faint radio sources, in particular to look for variations in the source counts and spectral-index distributions. Variations caused by observational effects were minimized by choosing similar declinations (32^o and 27^o) and similar galactic latitudes (-27^o and 30^o) for the two surveys.

The instrument and method of observation were identical to those of 5C5 (Pearson 1975); some relevant details are listed in Table 1. A few differences between the analyses of 5C5 and of 5C6 and 5C7 are noted in Section 2; the results are presented in Sections 3 - 10, and the conclusions are summarized in Section 11.

TABLE 1 Properties of the Surveys

		5C6	5C7
Right Ascension		$02^h\ 14^m$	$08^h\ 17^m$
Declination		32^o	27^o
Galactic Coordinates (l, b)		143.2, -27.3	196.2, 30.3
Epoch of observations		1973 Sep-Dec	1974 Jan-Mar
Noise level (mJy rms)	408	1.5	2.0
	1407	0.26	0.26
Number of sources detected	408	277	267
	1407	57	64

Synthesized Beam	408 MHz	1407 MHz
FWHM width	80"x80" cosec δ	23"x23" cosec δ
Radius of first grating ring	$3^o.6$x$3^o.6$ cosec δ	$1^o.0$x$1^o.0$ cosec δ
First sidelobe	-5.5 per cent of maximum	
First grating ring	5 per cent of maximum	
Envelope response		
FWHM width	150'x164'	48'
Width at 0.2 contour	226'x248'	74'

Assumed flux densities of calibration sources (Jy)
(Kellermann, Pauliny-Toth & Williams 1969: KPW)

3C 380	34	14.2
3C 147	42	22.2

2 Analysis

Because the TITAN computer of the University of Cambridge Computer Laboratory was no longer available, the analysis programmes used for 5C1 - 5 had to be modified and the significant changes are described in this section.

2.1 THE FOURIER TRANSFORM

The new programme was designed to employ a fast (factorized) Fourier transform algorithm in two dimensions. This requires the data to be sampled on a square grid in the baseline plane (that is, the plane in which aerial separation and hour-angle are polar coordinates), so interpolation from the polar to a Cartesian grid is required (Thompson & Bracewell 1974). The interpolation function chosen was such as to reduce all the 'alias' responses (introduced by the factorized Fourier transform) to less than 4 per cent, small enough to cause no problems even though the whole of the area could not be mapped in a single transform operation. Each map was constructed from six overlapping panels.

The 5C7 1407-MHz map was dominated by the source 5C7.118 (0816+268) so the response due to this source was removed from the data by the method of Neville, Windram & Kenderdine (1969). This reduced the rms fluctuation on the map from about 0.35 mJy to 0.26 mJy. There are three strong sources near the centre of the 5C7 408-MHz field, and the sidelobes of these, together with some low-level terrestrial interference, account for the difference between the rms noise levels of 5C6 and 5C7. These three sources are too close together to be successfully removed by the visibility-averaging procedure of Neville *et al.*, but some clarification of the map was achieved by subtracting their ideal responses.

2.2 BEAMSHAPE FITTING

The beamshape-fitting programme differed from the original in that it determined positions and flux densities independently - the position by locating the half-power points of the response, and the intensity by a least-squares fit to the beamshape at the estimated position (Gillespie 1974). In 5C6, the 408-MHz positions were corrected by adding $0^s.3$ ($\pm 0^s.1$) to the right ascensions and 3" ($\pm$1") to the declinations, the corrections being derived by comparison of the 408-MHz and 1407-MHz positions of 24 unresolved sources. In 5C7, the mean positions at the two frequencies were not significantly different ($\Delta\alpha = 0^s.09 \pm 0^s.05$, $\Delta\delta = 1".4 \pm 2".4$, 27 sources) so no corrections were made.

The uncertainties in the fitted parameters were estimated by the usual method of adding artificial sources to the maps. The uncertainty in the position of a source varies inversely as its

signal-to-noise ratio, and the uncertainty in flux density is consistent with the estimated noise level. Systematic errors in the positions and flux densities will be discussed in Section 5.

2.3 RESOLVED SOURCES

At 1407 MHz, a second map of each surveyed area was made from the small-baseline observations, with FWHM beamwidth 70 arcsec, again using a truncated Gaussian grading. The beamshape-fitting programme was used to find the sources on this map brighter than 5σ. All of these could be identified with sources on the high-resolution map, and for each of them the ratio $r = S_h/S_l$ was computed, where S_h = flux density at high resolution, S_l = flux density at low resolution. Those for which r was significantly greater than 1 were regarded as extended, and for them S_l was adopted in preference to S_h. Few of the sources appeared to be resolved by the 70-arcsec beam; a large proportion, however, were resolved by the 23-arcsec beam - in 5C6, 12 of the 39 sources found on both maps were resolved at the 2σ level, and in 5C7, 12 out of 39 sources were resolved. Thus at least 30 per cent of sources are resolved by the 23-arcsec beam and have angular sizes $\gtrsim$ 15 arcsec, which is consistent with the suggestion by Katgert (1976) that 50 per cent of sources brighter than 10 mJy at 1415 MHz are larger than 10 arcsec. The 2σ criterion used here is restrictive - there will certainly be more sources which are extended but which are too faint for one to estimate r accurately. S_l was also adopted for a few sources clearly resolved on the contour map although not by the r-criterion.

A more elaborate version of this method has been used by Katgert (1975, 1976) to analyse Westerbork observations at 1415 MHz of the 5C2 region. He investigated the dependence of flux density on beamwidth for model double sources, and found empirically that the best estimate of flux density was $S_h^{-0.1}S_l^{1.1}$. As this result depends on the properties of the individual maps and the source model used, it is not directly applicable to 5C so we have ignored the small dependence on S_h and simply used S_l if it was significantly different from S_h. This will lead to a general underestimation of flux densities which must be allowed for when computing the source count.

At 408 MHz, low-resolution maps (FWHM beamwidth 240 arcsec) were also made but, with an rms noise of about 6 mJy, they were too confused for the beamshape-fitting programme to run successfully. The flux densities of extended sources were estimated instead by integration, and were checked by means of a beamshape-subtracting programme (similar to CLEAN, Högbom 1974). For strong sources, the sum of the subtracted components agreed quite well with the result of the integration, but for weak (< 10σ) or very extended sources both methods were unreliable. In the few cases in which it was possible, the apparent flux densities measured

from the low-resolution map were also considered.

3 Source lists

Table 2 lists all the sources detected in the 5C6 survey whose flux densities before envelope correction (S') were greater than 10.0 mJy (408 MHz) or 1.5 mJy (1407 MHz), and Table 3 lists all the 5C7 sources with S' greater than 12 mJy (408 MHz) or 1.6 mJy (1407 MHz). These limits are approximately 6σ. The 408-MHz flux densities of some sources below these limits are also included (in parentheses).

The format of Tables 2 and 3 is as follows:

Column

1 Serial number; the sources in each survey are numbered in increasing order of right ascension. Occasionally two sources are grouped together in the lists, and given suffixes a, b; this is done either when there are two peaks of emission at 1407 MHz but only one at 408 MHz, or when there is an obvious association between the two sources.*

2 Right Ascension (1950.0).

3 Declination (1950.0).
Positions measured at 1407 MHz are distinguished by an extra decimal place in columns 2 and 3.

4 rms uncertainty in right ascension (arcsec), excluding any systematic error; the uncertainties in declination are greater by cosec δ. 'e' means that the source is extended and the position given is the peak of emission.

5 Flux density at 408 MHz, S_{408} (mJy).

6 rms uncertainty in S_{408} (mJy), including contribution of 3 per cent uncertainty in the envelope correction.

---

* We have not adopted the nomenclature recommended by IAU Commission 28 (*IAU Proceedings* 1973, page 142) because this position-based system would be ambiguous for some of the 5C sources which are very close together. In the absence of an established practice for such cases, we feel that our adherence to an established nomenclature will cause less confusion than the introduction of a new one. We recommend, however, that when it is necessary to refer to a source by its 5C name in a context in which its position is not obvious, the 5C name should be accompanied by the IAU name in parenthesis, thus: 5C7.103 (0815+266).

7 Envelope attenuation factor at 408 MHz (multiply S by this factor to recover S' and hence the signal-to-noise ratio).

8 Flux density at 1407 MHz, S_{1407} (mJy). A '+' in this column indicates that although the position was measured at 1407 MHz, the flux density could not be determined.

9 rms error in S_{1407} (mJy).

10 Envelope attenuation factor at 1407 MHz.

11 Spectral index $\alpha(408,1407)$ defined by $S \propto \nu^{-\alpha}$.

12 Notes, including descriptions of optical objects within 15–20 arcsec. The parameter r (Section 2) is given for sources detected at 1407 MHz on both high- and low-resolution maps; r * means that r could not be determined accurately. The following abbreviations are used: conf = confused, sl = slightly, pa = position angle; and for the optical objects: N = North, S = South, f = following, p = preceding, m = magnitude. The references to other observations are as follows:

3C	Third Cambridge Catalogue (3C 200 only)
4C	Fourth Cambridge Catalogue (Pilkington & Scott 1965)
AO	Arecibo Occultation survey (Hazard, Gulkis & Sutton 1968)
B2	Bologna survey (Colla *et al.* 1970, 1972, 1973)
GC	NRAO 5-GHz survey (Davis 1971)
MW	One-Mile Telescope fan-beam survey (Willson 1972b)
PKS	Parkes Survey (Shimmins & Day 1968)
W	Westerbork 1415-MHz survey (Willis, Oosterbaan & de Ruiter 1976)
5-km	observations with the 5-km telescope (Section 4.4).

An asterisk '*' in column 6 or 9 indicates that the uncertainty in flux density is very large because the source lies outside the measured part of the envelope (attenuation factor less than 0.1 at 408 MHz or 0.15 at 1407 MHz). These sources are included in the tables only for their positions; many of them have been observed in other surveys so it is possible to check the positional accuracy (see Section 5).

4 Comparison with other surveys

4.1 THE BOLOGNA B2 SURVEY, 408 MHz

Both 5C6 and 5C7 lie in the region covered by the B2 survey (Colla *et al.* 1970, 1972, 1973), and a comparison of the sources in common provides a useful check on the scaling and linearity of the flux densities. The resolution of the B2 survey (FWHM 3 x 10 arcmin) is adequate to identify the B2 sources unambiguously with sources in the 5C surveys.

(a) 5C6

Most of the 5C6 region falls within the area of the B2.1 survey ($29^{\circ}18' < \delta < 34^{\circ}02'$) in which the B2 flux density limit is 0.20 Jy; the remainder is covered by B2.2 and B2.3 to 0.25 Jy. All of the B2 sources in the region surveyed were detected, with the exception of three (0205+29, 0221+29, 0224+29) which lie at the edge of the field of view where the sensitivity of 5C6 is less than that of B2; B2 0211+30A was found to be a blend of 5C6.74 and 75, in agreement with the note in the B2 catalogue that it is 'possibly complex N-S'. Most of the 5C6 sources brighter than the B2 limit are listed in the B2 catalogue. Of those that are not, four (5C5.1,3,5,251) are at the edges of the 5C6 field, and their flux densities are perhaps overestimated; the remaining two (5C6.114 and 214) are at declinations ($34^{\circ}06'$, $34^{\circ}09'$) close to the boundary of B2.1 and B2.3 where the B2 catalogue may be incomplete.

A sample of 23 sources was selected, consisting of all the sources in common within the 10 per cent contour of the envelope and neither resolved nor confused in 5C6. The mean difference in positions (B2-5C6),

$$\overline{\Delta\alpha} = -0^{s}.55 \pm 0^{s}.15 = -7.0 \pm 1.9 \text{ arcsec}, \quad \sigma_{\alpha} = 9.4 \text{ arcsec},$$

$$\overline{\Delta\delta} = 0.01 \pm 0.13 \text{ arcmin}, \quad \sigma_{\delta} = 0.61 \text{ arcmin},$$

indicates a shift of one system relative to the other in right ascension. Independent evidence (Davis 1971; Pauliny-Toth, Witzel & Preuss 1974) suggests that the B2 right ascensions should be increased by $0^{s}.3 \pm 0^{s}.1$; with this correction, the difference between B2 and 5C6 is not significant.

The flux densities of the 23 sources are compared in Fig. 1(a); there is no evidence for any non-linearity in either 5C6 or B2. The mean ratio of the flux densities is 1.00 ± 0.03; that is, the scale of 5C6 is the same as that of B2 (which is 4 ± 2 per cent higher than KPW), and not significantly different from the KPW scale that the calibration was intended to achieve. There is no marked dependence of the ratio $S(5C6)/S(B2)$ on either declination or right ascension, indicating that the 5C6 envelope correction introduced no errors greater than 5 per cent for sources within the 10 per cent contour. The resolved sources within the 10 per cent contour show a wider scatter of the flux density ratio, but there is again no disagreement between 5C6 and B2. The sources outside the 10 per cent contour show a tendency for the 5C6 flux densities to be overestimated by up to 10 per cent; this is not surprising as the envelope was not accurately measured in this region.

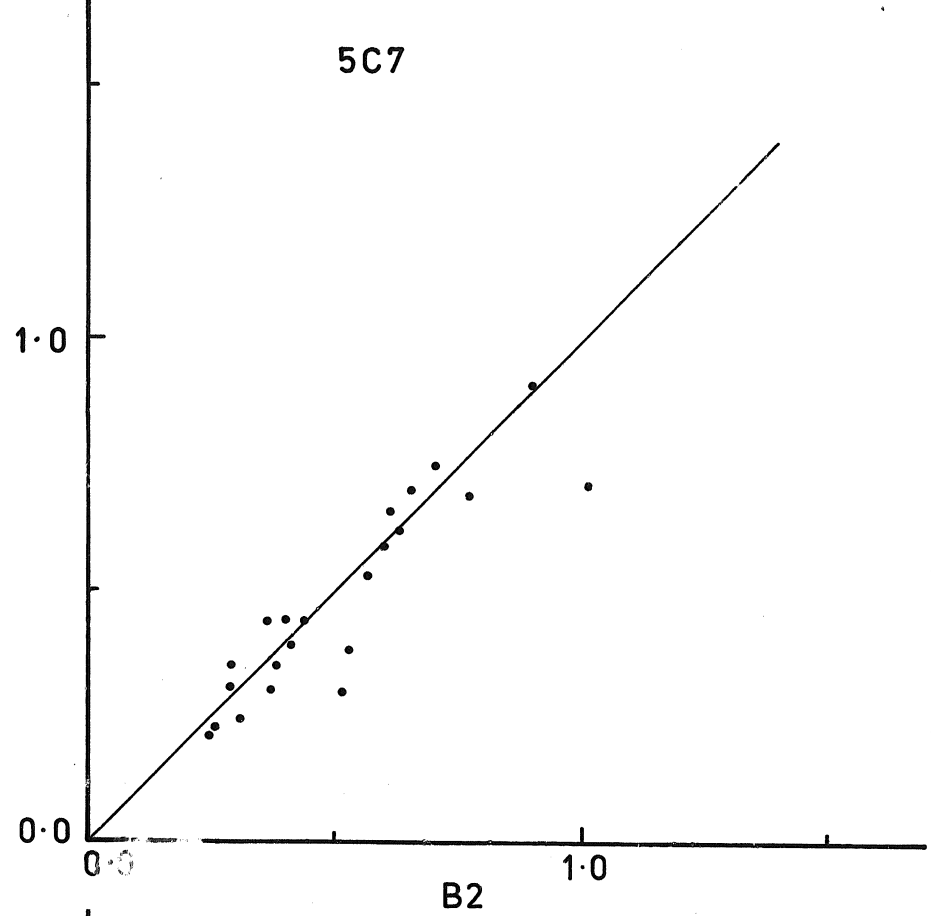

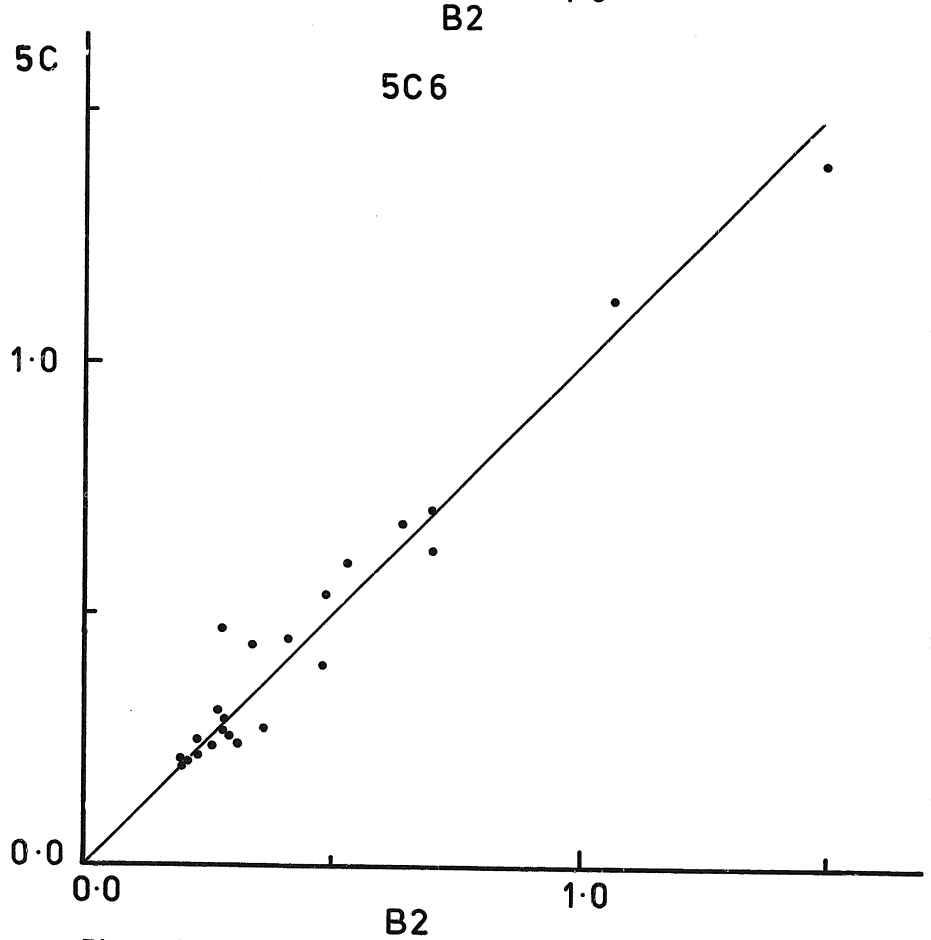

Figure 1. Comparison of 408-MHz flux densities measured in (a) 5C6 and (b) 5C7 and in the B2 survey. The straight lines have unit slope; the scales show S_{408} in Jy.

(b) 5C7

5C7 lies in the B2.2 area ($24^{\circ}02' < \delta < 29^{\circ}30'$) where the B2 limit is 0.25 Jy. 40 B2 sources were detected in 5C7, of which 22 lie within the 0.1 contour of the envelope. The only B2 source within the 0.1 contour that was not detected is B2 0808+26B, which is a blend of 5C7.11 and 5C7.12. There are three 5C7 sources stronger than 0.25 Jy but not listed in B2. The flux densities are compared in Fig. 1(b); the mean ratio of the flux densities of the 22 sources (B2/5C7) is 1.06 ± 0.04, consistent with the assertion that B2 is 4 per cent higher than the 5C (KPW) scale. The mean positional differences (B2-5C7) are:

$$\overline{\Delta\alpha} = +0^{s}.22 \pm 0^{s}.15 = 2.9 \pm 2.0 \text{ arcsec}, \quad \sigma_{\alpha} = 9.5 \text{ arcsec},$$

$$\overline{\Delta\delta} = 0.12 \pm 0.15 \text{ arcmin}, \quad \sigma_{\delta} = 0.69 \text{ arcmin}.$$

4.2 COMPARISON OF 5C7 WITH THE WESTERBORK SURVEY, 1415 MHz

Part of the 5C7 region was observed at Westerbork by Weiler *et al.* (1974) in an unsuccessful search for low-brightness emission around the pulsar AP 0823+26, and a catalogue of the background sources detected in the field is given by Willis *et al.* (1976). The Westerbork field falls entirely in the eastern part of the 5C7 field, and there is no overlap with the 5C7 1407-MHz observations. The two surveys are compared in Table 4. The spectral-index distribution derived from these sources agrees reasonably well with the distributions derived from the 5C observations alone (see Section 10): the median $\alpha(408,1415)$ is 0.78.

Ten of the Westerbork sources were detected above the 6σ limit of 5C7. The positional agreement is good, with the exception of two sources near the edge of both fields (0824+27W1 and 0824+26W3) for which the disagreement is greater than 10 arcsec. Excluding these two, the mean differences (Westerbork - 5C7) are:

$$\overline{\Delta\alpha} = 0^{s}.09 \pm 0^{s}.06 = 1.2 \pm 0.9 \text{ arcsec}, \quad \sigma_{\alpha} = 2.5 \text{ arcsec},$$

$$\overline{\Delta\delta} = -1.4 \pm 1.2 \text{ arcsec}, \quad \sigma_{\delta} = 3.4 \text{ arcsec}.$$

Even if the two anomalous sources are included, the differences are not significant.

4.3 OTHER SURVEYS

Table 5 lists the 5C6 and 5C7 sources detected in several other surveys. The positions are generally in good agreement with the earlier measurements.

TABLE 4 The sample of Westerbork sources in the 5C7 area

Westerbork	5C7	S_{408} (mJy)	S_{1415} (mJy)	$\alpha(408,1415)$	Identification
0822+26W1	237	207	58.3	1.02	
0822+26W2	238	35	20.3	0.44	
0822+27W1	243	156	99.0	0.37	Stellar, B=18.5
0822+26W3	245	685	215.1	0.93	
0833+27W1	251	53	19.8	0.79	
0823+26W1	252	127	42.7	0.88	
0823+26W2	255	94	37.9	0.73	
0823+26W3	-	34	15.9	0.61	
0824+26W1	-	<24	9.4	<0.75	
0824+26W2	264	175	97.2	0.47	Stellar, B=20.5
0824+27W1	265	63	18.3	0.99	
0824+26W3	268	67	19.9	0.99	
0825+26W1	-	*			

* Outside 0.1 contour of envelope

The identifications are from de Ruiter, Willis & Arp 1977;
the limiting magnitude was B=22.5.

TABLE 5

Other observations of 5C6 and 5C7 sources

	B2 name	Other names	References
5C6			
4	0204+32	4C 32.10	(3),(10)
5	-	GC 0204+33	(1),(2)
8	0204+31		(3),(10)
19	0206+33	GC 0206+33	(1),(2),(3),(10)
62	0210+32	GC 0210+32	(1)
160	0214+33	GC 0214+33	(1)
211	-	GC 0216+33A	(1),(2),(5)
217	0216+33B	GC 0216+33B	(1),(2),(3),(10)
237	0217+32		(3),(10)
258	0219+33A	GC 0219+33	(1)
288	0222+31C		(3),(10), spectrum in (9)
5C7			
6	0807+27	4C 27.18	(3),(6),(7)
9	0808+24		(3)
70	0814+29A	4C 29.28a	(3),(4),(7)
78	0814+29B	4C 29.28b	(3),(4)
111	0816+26A		(3)
118	0816+26B		(6)
178	0818+29		(7)
195	0819+28		(6)
205	0820+24A		(3)
214	0820+29		(7),(8)
261	0824+29	3C 200	(3),(7)
270	0825+24	4C 24.17	(3)

References:

(1) Davis 1971
(2) Pauliny-Toth, Witzel & Preuss 1974
(3) Grueff & Vigotti 1973
(4) Grueff & Vigotti 1975
(5) Fanti *et al.* 1974
(6) Fanti *et al.* 1975
(7) Ghigo & Owen 1973
(8) Wills & Wills 1976
(9) Gearhart, Kraus & Andrew 1976
(10) Warwick 1977

TABLE 6

5 km Telescope Observations of 5C5, 5C6 and 5C7 sources

	Date	Frequency	RA	Dec	Flux density (mJy)	$\overline{\Delta\alpha}$ (5C - 5 km) (s)	$\overline{\Delta\delta}$ (5C - 5 km) (arcsec)	
5C5.9	750719	5 GHz	09 30 18.35	49 03 25.8	150	0.15	-12.8	Unresolved
(5C1.7)						1.45	-4	
5C5.14	*	5 GHz	09 30 55.5	49 21 43.6	42	-0.5	10	
(5C1.12)						1.3	-7	
5C5.131	730914	5 GHz	09 40 20.12	46 47 17.7	78	-0.01	0.1	Unresolved
5C6.78	760708	2.7 GHz	02 11 07.74	32 36 05.2	-	-	-	See Section 7
5C6.88			02 11 29.62	32 38 08.7	-	-	-	(peak positions)
			02 11 30.15	32 38 12.6				
5C7.118	760525	2.7 GHz	08 16 15.00	26 51 29.5	150	0.03	-1.0	Double
			08 16 15.46	26 51 24.2		-0.43	4.3	

* From Gillespie 1977.

4.4 5-km TELESCOPE OBSERVATIONS

A number of 5C sources have been observed with the Cambridge 5-km telescope (Ryle 1972), either for their intrinsic interest or to check the One-Mile telescope positions. The results of these observations are summarized in Table 6; some of the sources will be described more fully in Section 7. The FWHM beamwidth of the 5-km telescope is 2 arcsec at 5 GHz and 3.7 arcsec at 2.7 GHz.

5 Systematic errors in the 5C surveys

5.1 FLUX DENSITY

The comparison (Section 4.1) of the 5C6 and 5C7 flux densities with those from the B2 survey and the comparison (Pearson 1975) of 5C5 with a Half-Mile telescope survey (Gillespie 1975, 1977) show that there are no gross scaling or envelope-correction errors in the 5C surveys at 408 MHz within the measured part of the envelope. The radial variation of the flux-density scale in 5C1 and 5C2 noticed by Condon & Jauncey (1973) is not found in the new surveys.

5.2 POSITION

Some evidence has accumulated that there are systematic errors in the positions measured in the earlier 5C surveys. These are of two types: (i) errors in the position of the *map-centre*, which affect all sources equally and which can be attributed to errors in the calibration of the telescope or to tropospheric or ionospheric refraction, for example; and (ii) *marginal errors*, that is, errors in the measurement of source positions relative to the map-centre, which are greatest at the margins of the map. To first order, these look like a rotation or stretching of the entire field of view; they could be attributed to (implausible) frequency or baseline errors, to timing errors, or to errors in the precession corrections. The evidence for errors of the two types is summarized in Tables 7 and 8.

During the analysis of 5C6 and 5C7, an error was found in the computation of the hour-angle of the first recorded sample, and hence in the orientation of the maps. The hour-angle is 12^{s} earlier than that recorded, on account of the signal delay in the post-detector amplifiers. This mistake has been corrected in 5C6 and 5C7, but it affects 5C5 and the earlier surveys. (No allowance was made for this time-constant in the TITAN programmes.) The error is equivalent to a rotation of 3 arcmin in the equatorial plane, giving position errors of up to 20 arcsec at the edges of the maps. If this were the only source of error, however, all the rotations in Table 8 should have the same sense, which is not the case.

Errors can be detected by comparing the measured positions

TABLE 7

Estimates of Systematic Map-centre errors in the 5C Surveys

Survey	Comparison survey	$\overline{\Delta\alpha}$ (s)	$\overline{\Delta\delta}$ (arcsec)	σ_α (s)	σ_δ (arcsec)	
5C1	ARG	+0.39 ± 0.023	-0.07 ± 1.32	0.65	0.35	Gillespie 1974
5C2	ARG	-0.25	-2.5 ± 1.1			Gillespie 1974
	Optical	0.01 to 0.09	-3			Notni *et al.* 1971
5C3	Westerbork		+3			van der Kruit & Katgert 1972
	NRAO	+0.08 ± 0.12	+3.7 ± 1.1	0.37	3.4	Spencer & Burke 1975
	Optical	-0.24 ± 0.70	+1.22 ± 1.05			Parkes & Penston 1973
5C4	ARG	-0.33 ± 0.087	-3.29 ± 1.76	0.63	12.6	Gillespie 1974

Notes

ARG refers to a Half-Mile Telescope survey made by Gillespie
The differences $\Delta\alpha$ and $\Delta\delta$ are computed in the sense (5C survey minus comparison survey)

TABLE 8

Marginal errors in the 5C Surveys

5C1	Comparison with Half-Mile Telescope Survey Right ascension scale compressed by 0.12±0.05 per cent. No evidence for rotation.	(Gillespie 1974)
5C2	Comparison with optical positions Right ascension scale compressed by 0.12 per cent.	(Notni *et al.* 1971)
	Comparison with Half-Mile Telescope Survey Right ascension scale compressed by 0.18±0.09 per cent. Possible rotation < 5 arcmin.	(Gillespie 1974)
	Comparison with Westerbork 1415 MHz Survey Right ascension scale error and rotation, attributed by Katgert to omission of the differential precession correction.	(Katgert 1975)
5C3	Comparison with optical positions Right ascension scale compressed by 0.12 per cent.	(Richter *et al.* 1974)
	Right ascension scale expanded by 0.004±0.019 per cent. Declination scale compressed by 0.088±0.030 per cent.	(Parkes & Penston 1973)
5C4	Comparison with Half-Mile Telescope Survey No evidence for right ascension scale error. Rotation by (4±3) arcmin in opposite sense to 5C2.	(Gillespie 1974)

with more accurate ones (either radio or optical) for a large sample covering the whole field of view. In 5C6 and 5C7 we have the two B2 samples, which place limits of about 5 arcsec on any error in the right ascension of the map-centre; in 5C7, the Texas observations place limits of about 2 arcsec on the right-ascension error, and the other measurements limit the declination error to about 4 arcsec. From the right ascensions of the B2 survey and the accurate declinations obtained in the observations listed in Table 5, we can place the following limits:

(i) on rotation of the maps (regarded as a rotation in the projection on the equatorial plane): less than 1 arcmin in both surveys;

(ii) on stretching of the maps: in both surveys, the right ascension scale error is less than 0.06 per cent ($0^s.04$/min) but a declination error is harder to detect. For 5C7, the Westerbork survey can be used: if the $\overline{\Delta\alpha}$ and $\overline{\Delta\delta}$ of Section 4.2 are interpreted purely as marginal errors (no map-centre error), the right ascension scale error is 0.03 ± 0.02 per cent, and the rotation 0.45 ± 0.39 arcmin.

These limits are less stringent than we should like, but for 5C6 and 5C7 they rule out errors as large as those found in some of the earlier surveys, e.g. the right ascension scale error of $0^s.07$/min found in 5C2 and 5C3 by Notni *et al.* (1971) and Richter *et al.* (1974), and the puzzling errors found in 5C2 by Katgert (1975). The situation for 5C5 is unclear: in particular, a discrepancy in the right ascensions between 5C5, 5C1 and ARG suggests that there is a map-centre error in 5C5. But because all the sources common to the three surveys lie in the northern part of 5C5, it is impossible to distinguish a map-centre error in right ascension from a rotation, and the differences can equally well be attributed to the latter (possibly accompanied by a rotation of 5C1 in the same sense); the required sense and approximate magnitude of the rotation correspond to the time-constant error discussed above. Further accurate observations are required, particularly of sources in the southern part of 5C5, to distinguish the possibilities. The one accurate position available for a source near the centre of 5C5 (5C5.131, Table 6) agrees well with the 5C position, making a rotation more plausible than a shift.

6 Optical identification

The two authors have independently examined prints of the Palomar Sky Survey using transparent overlays to locate the radio source positions. Brief descriptions are given in column 12 of Tables 2 and 3 of optical objects which we *both* could see within about 20 arcsec of the radio positions. The list of optical objects is not intended to be complete to the print limits, and it is hoped

that this preliminary study will be supplemented by more accurate measurements, preferably on deeper plates. A comparison of our estimates of the magnitudes of the candidate objects suggests that the standard error is about 0.5 mag.

5C6

Eight galaxies from the Morphological Catalogue of Vorontsov-Vel'yaminov & Arkhipova (1964; MCG) are noted in Table 2; in addition, emission below the completeness limit of the survey was noticed for MCG 5-6-18 ($S_{408} \approx 10$ mJy) and MCG 5-6-31 ($S_{408} \approx 8$ mJy). Of these ten galaxies, seven are spirals, the others being either elliptical or 'compact'. The 14 mag galaxy MCG 5-6-17 (5C6.98) is curious: the radio source is extended over ≈ 4 arcmin, and the galaxy lies in one of the two 'arms' of the source. It is possible that only this arm is associated with the galaxy, the remainder being an unrelated object. There are no obvious associations with catalogued clusters, but several of the sources appear to lie in groups of galaxies.

5C7

One galaxy from the Morphological Catalogue was identified with a source in 5C7: MCG 5-20-8 = 5C7.102a; emission below the survey limit was noticed for MCG 5-20-5 (spiral) and MCG 4-20-55 (elliptical), both ≈ 10 mJy.

7 Notes on individual sources

Contour maps of some of the sources resolved by the 1407-MHz beam are shown in Figs 2 and 3. Notes on some of these and on others follow.

5C6.78 and 88 (0211+326)

These two are among the strongest sources in the 5C6 area, and are clearly the two outer components of a double source (Fig. 4). At 408 MHz both components are slightly resolved in the axial direction, and there is an apparent central component between the two. The flux densities are: Eastern component, 710 mJy; central component, 100 mJy (not listed in Table 2); Western component, 560 mJy. At 1407 MHz the tails of the two outer components can be distinguished, but the central component is not visible. The source is, unfortunately, at the extreme edge of the 1407-MHz field of view where the survey is not very sensitive, and the 1407-MHz flux densities cannot be estimated. A 2.7-GHz map was made from a 12-hr observation with the 5-km telescope (Fig. 5 and Table 6); this observation was insensitive to structure on a scale $\gtrsim 1$ arcmin, so it was not possible to estimate the total flux density. There is no compact central component ($S_{2700} < 5$ mJy) - it appears that at 408 MHz the 'central component' is really a bridge of extended

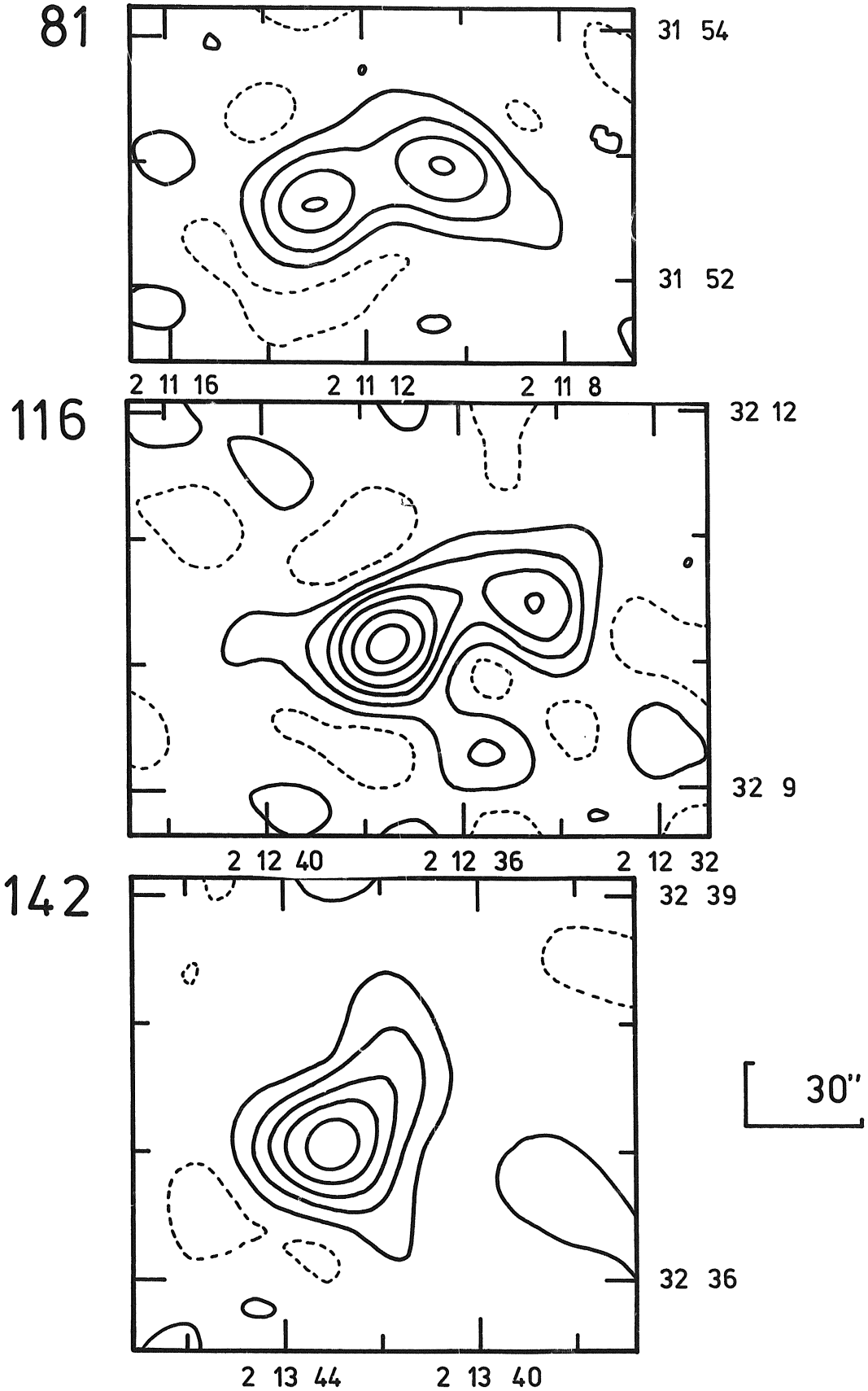

Figure 2. Contour maps of some 5C6 sources observed at 1407 MHz. The contour interval is 0.58 mJy in S' for all the diagrams and the dashed lines are negative contours.

B06

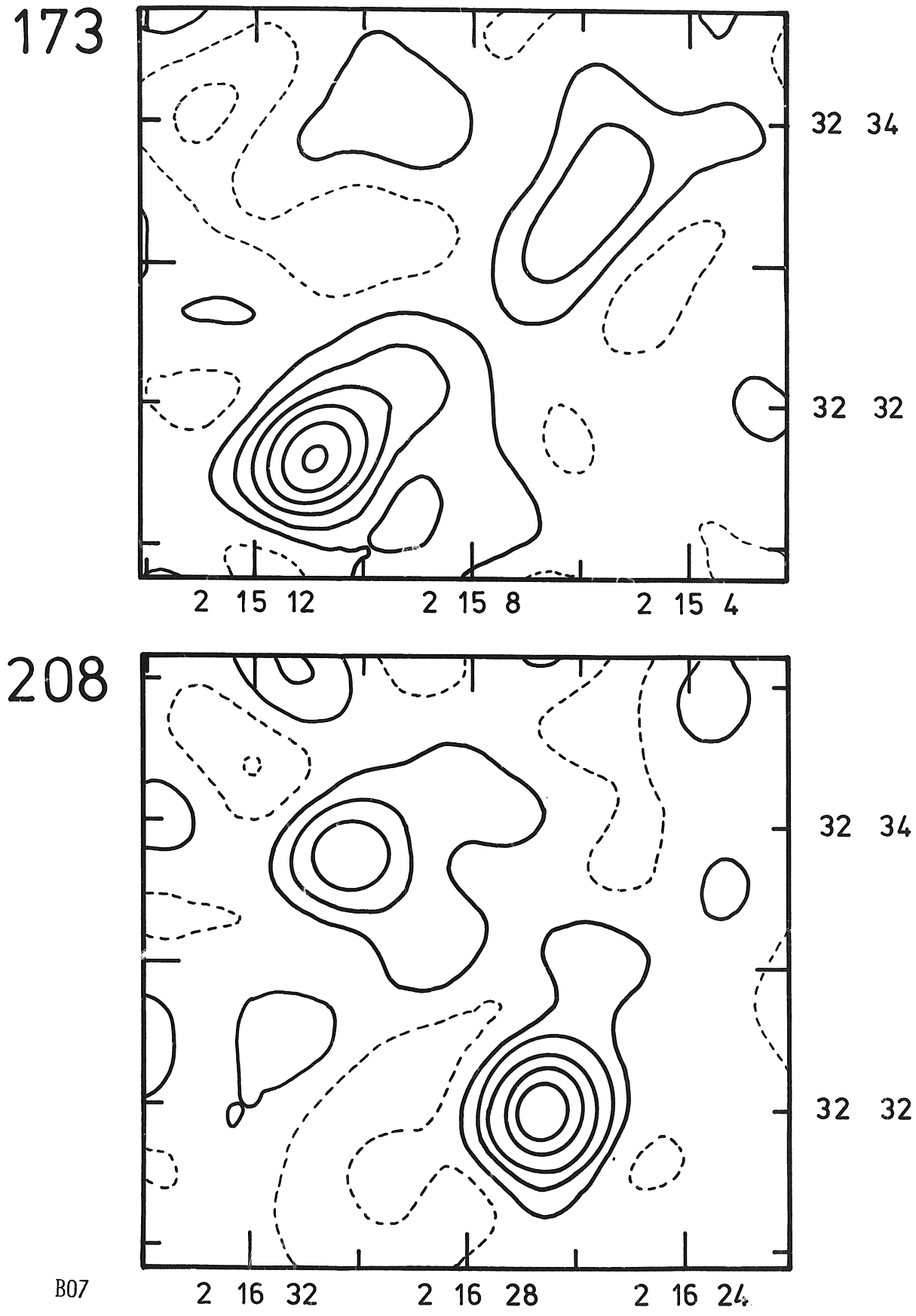

B07

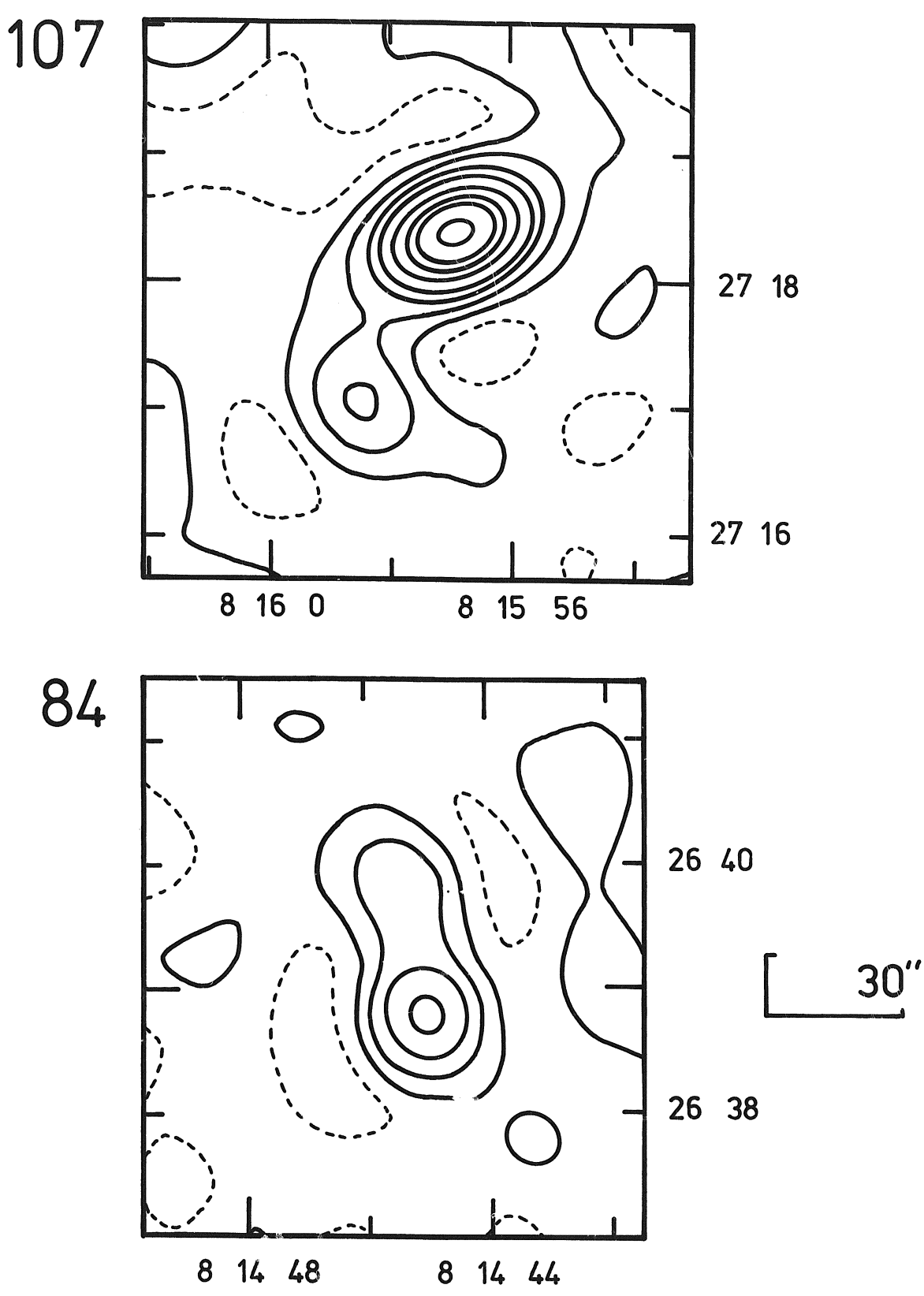

Figure 3. Contour maps of some 5C7 sources observed at 1407 MHz. The contour interval is 0.63 mJy in S' for all the diagrams and the dashed lines are negative contours.

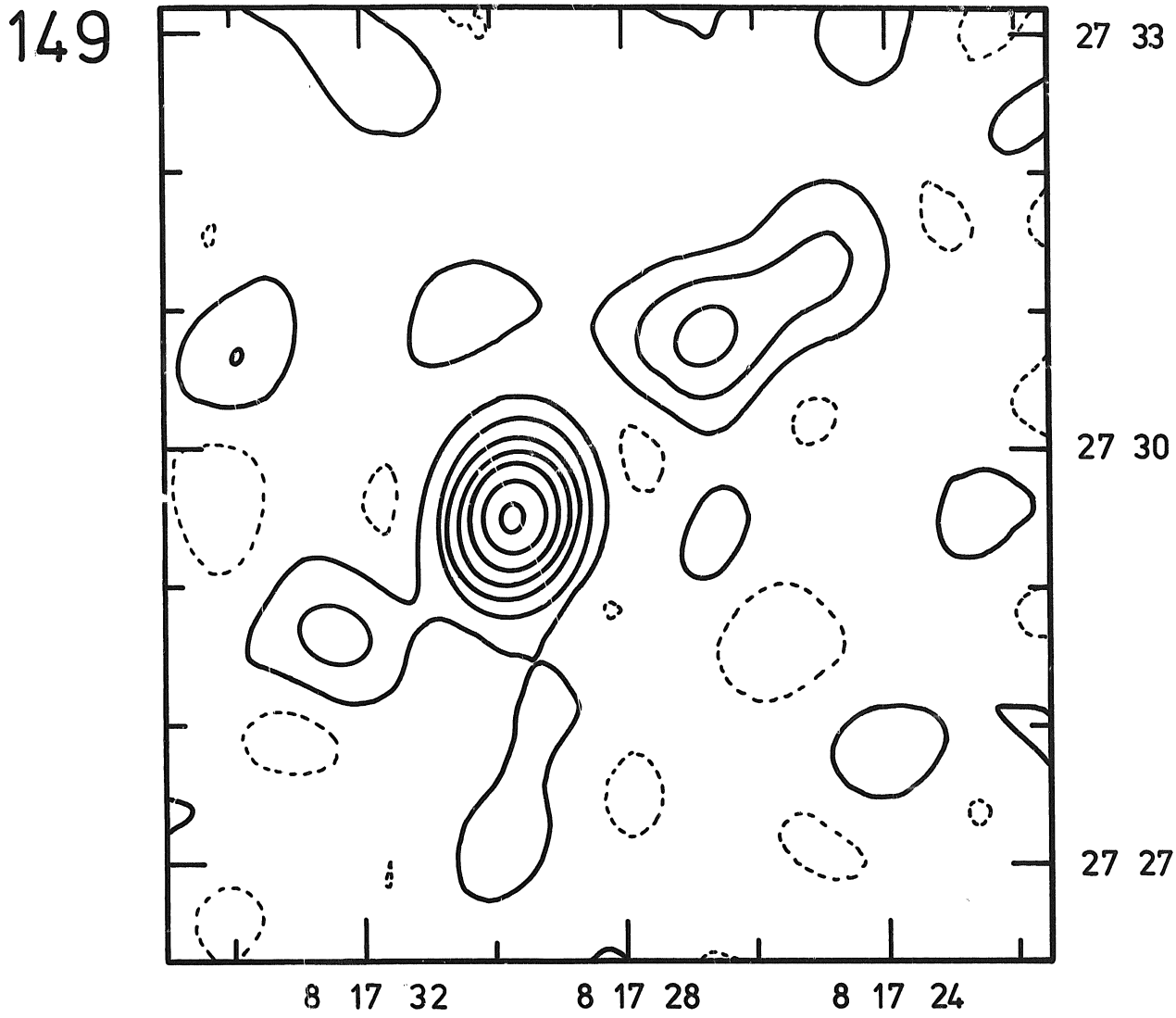

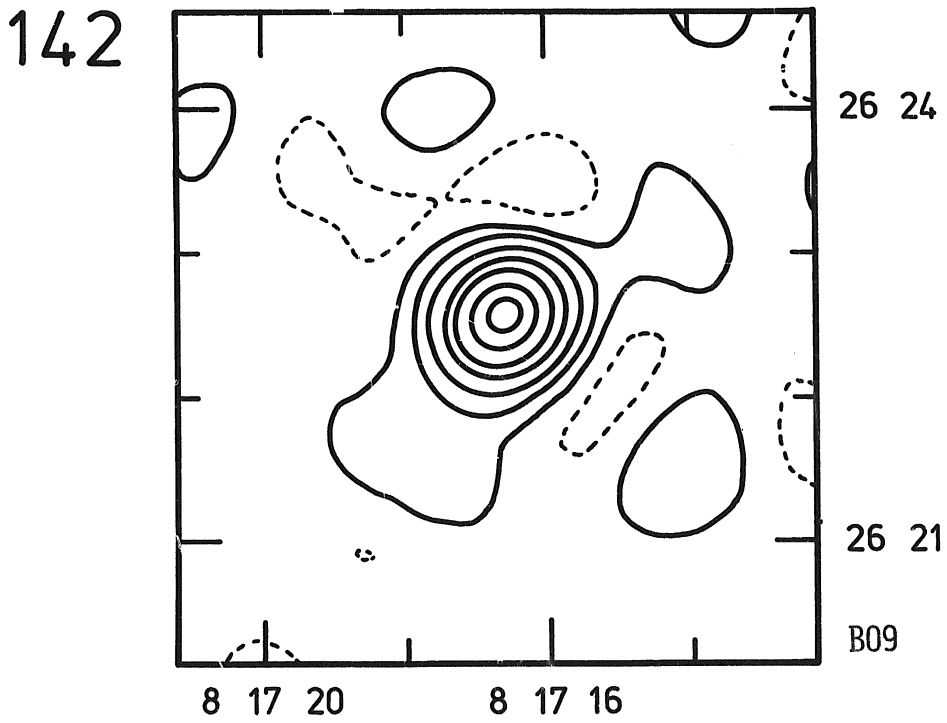

emission between the two outer components.

There is a 19.5 mag galaxy visible on the Sky Survey at the centre of the source; on the assumption that this is a typical giant elliptical galaxy associated with the source, the redshift is about 0.3. The component separation, 5.1 arcmin in p.a. 68°, corresponds at this redshift to a projected distance of 1.7 Mpc, and the total power of the source is P_{408} = 4.5 x 10^{25} W Hz^{-1} sr^{-1}. (H_0 = 50 km s^{-1} Mpc^{-1}; Einstein-de-Sitter world model). It is thus an unusually large source, but not an unusually luminous one.

5C6.142, 144 and 148 (0213+325)

These three sources could form a large extended source like 5C6.78 and 88; the two outer components (142 and 148) are both resolved at 1407 MHz, and on the low resolution 408-MHz map 144 forms an extended bridge between the other two. More sensitive observations will be necessary to reveal whether this association is real, but it illustrates the difficulty of determining the number of very extended ($\gtrsim$ 3 arcmin) sources in the 5C fields.

5C7.118 (0816+268)

This source is the most intense in the 5C7 1407-MHz field (before envelope correction) and was removed from the data before the Fourier transform. Its visibility at 1407 MHz was found to decrease with increasing baseline, indicating that it was slightly resolved, and this was confirmed by an observation at 2.7 GHz with the 5-km telescope which showed it to be double (Table 6). It is identified by Fanti *et al.* (1975) with an object having an ultra-violet excess (B = 18.2 mag) at α = 08 16 15.14, δ = 26 51 31.0; they give its angular size as 6 arcsec (at 5 GHz) in agreement with the 5-km observation. Its spectrum between 408 MHz and 5 GHz is straight, with spectral index 0.9.

5C7.256 = Pulsar AP 0823+26

The position of 5C7.256 is consistent with the precise position of AP 0823+26 obtained by pulse-timing (Reichley *et al.* 1973):
α = 08 23 50.52±0.02, δ = 26 47 18.1±0.8.
The total flux density, S_{408} = 84 ± 10 mJy, is rather larger than the mean pulsed flux density at 400-MHz, $\gtrsim$ 40 mJy (Manchester & Taylor 1972). It is not clear that this excess is associated with the pulsar, because the source appears to be slightly extended on the 408-MHz map, and the flux density estimate may be affected by confusion as well as the possible errors in the envelope correction so near the edge of the field of view.

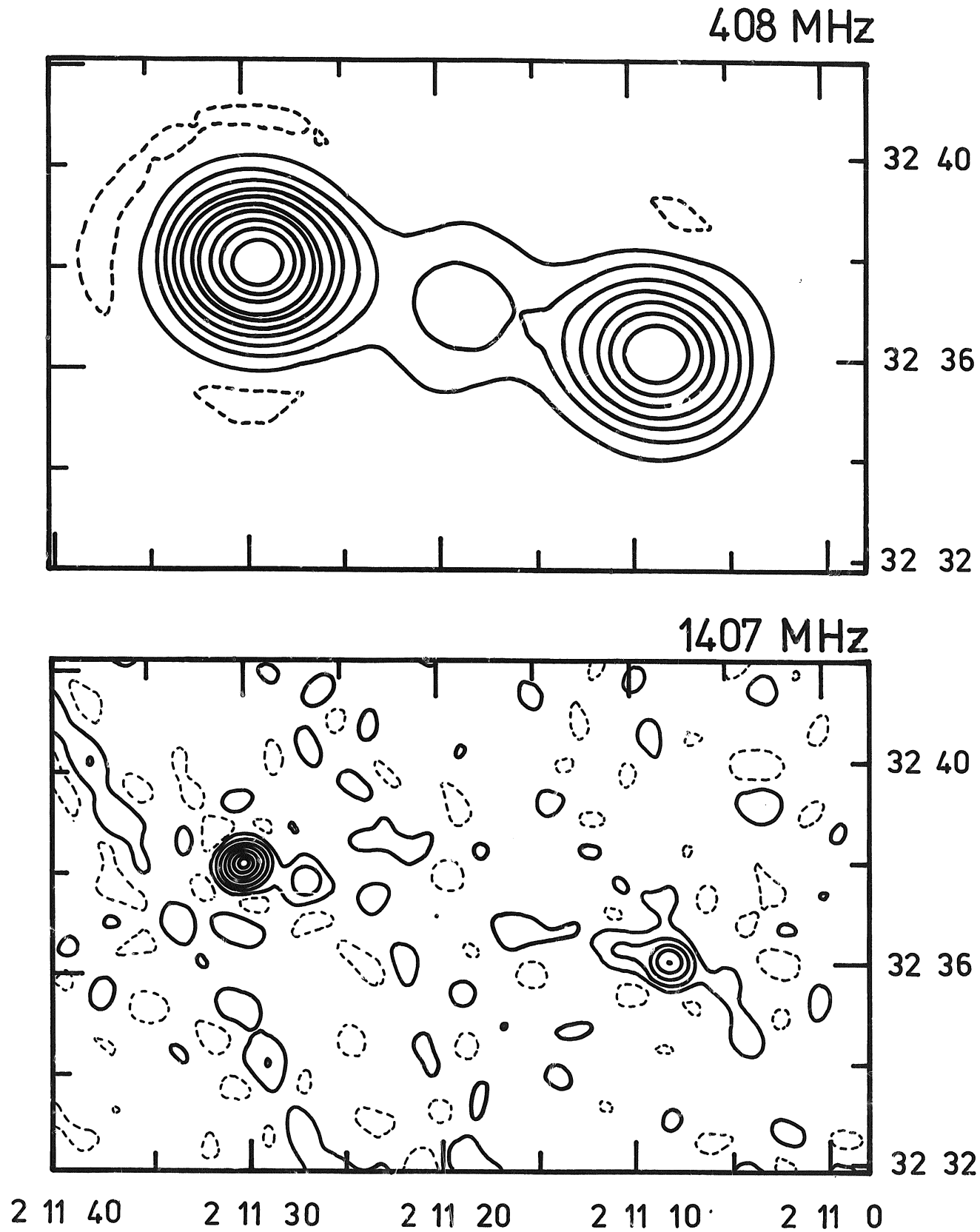

Figure 4. Contour maps of 5C6.78 and 88 at 408 MHz and 1407 MHz. The contour interval at 408 MHz is 60 mJy per beam area.

B11

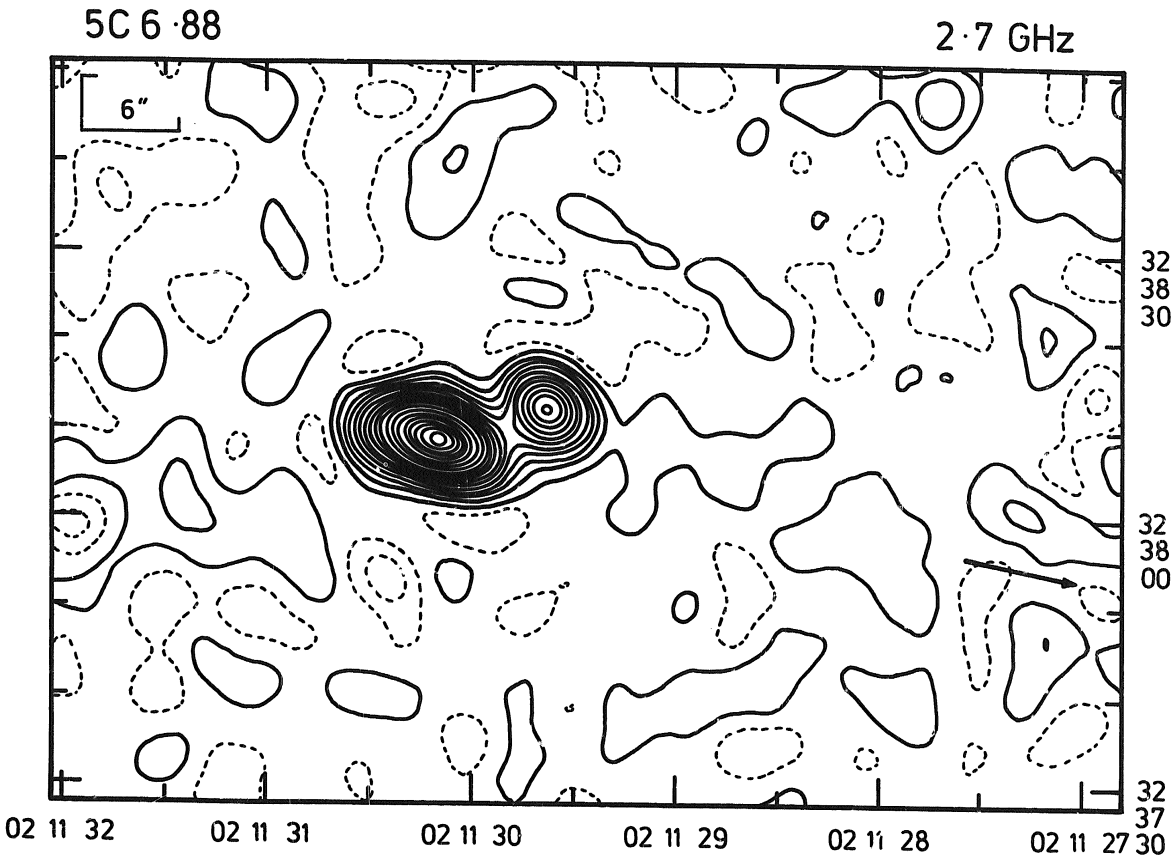

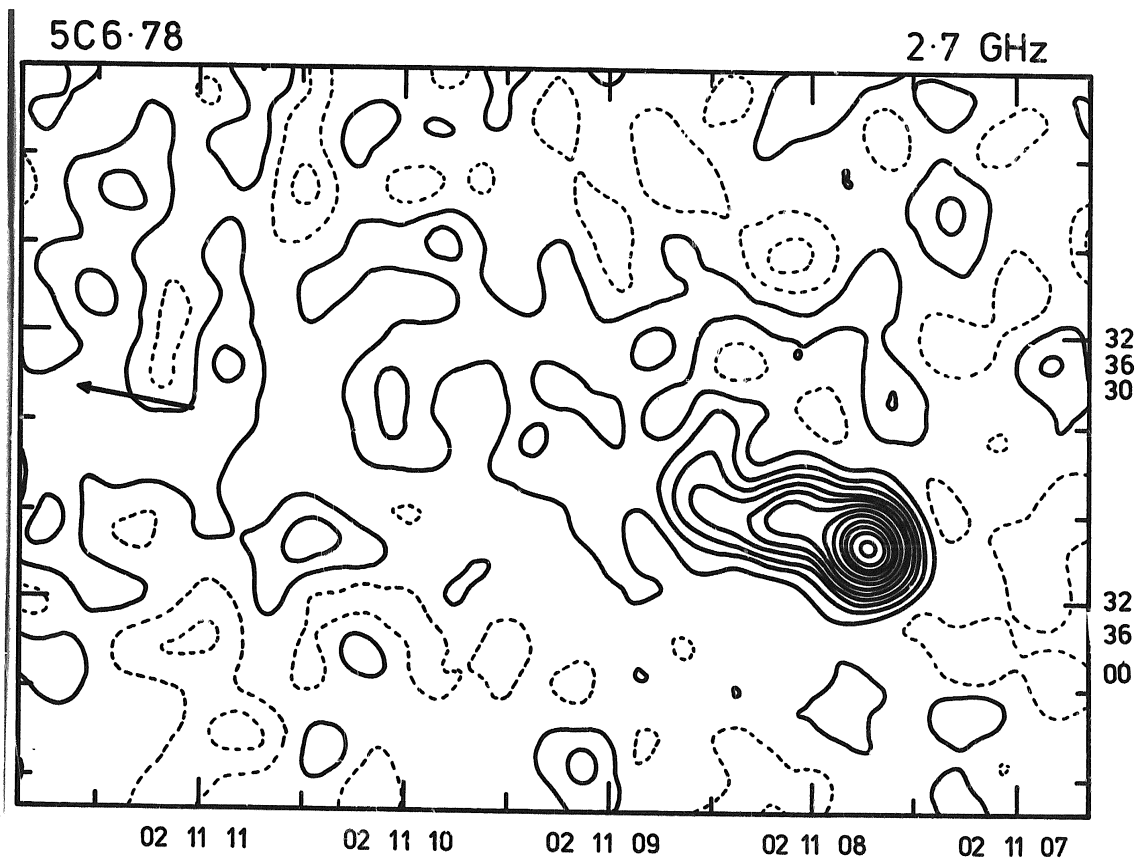

Figure 5. Contour maps of 5C6.78 and 88 at 2.7 GHz (5-km telescope). The contour interval is 2.5 mJy per beam area. The two arrows each point from the peak of one component to the peak of the other.

8 Source counts

8.1 408 MHz

The 408-MHz source counts from 5C6 and 5C7, computed in the same way as for 5C5, are presented in Table 9 and Fig. 6; the figure includes the 5C5 (Pearson 1975) and 5C2 (Pooley & Ryle 1968; Longair 1974) counts for comparison. The source counts were derived from the sources in each survey which lay within the 0.15 contour of the envelope and whose uncorrected flux densities S' exceeded 10.0 mJy (5C6) or 12.0 mJy (5C7).

5C6 and 5C7 have source densities generally higher than for 5C2 and 5C5, but the differences are not statistically significant. The surveys were compared by two χ^2-tests: in the first, the estimates of ΔN in five flux density ranges (defined by the 5C2 curve in Fig. 6) from each of the four surveys were compared, giving $\chi^2 = 23.1$ (15 degrees of freedom); in the second, nine flux density ranges were considered (as in Table 9) from each of the three new surveys, giving $\chi^2 = 21.3$ (17 degrees of freedom). Neither value of χ^2 is significant at the 5 per cent level and it can be concluded that there is no evidence for any significant differences between the survey areas, although it is worth noting that the two surveys closest to the Galactic plane (5C6 and 5C7, at latitudes $\gtrsim 30^{\circ}$) have the highest source densities - indeed, at least one of the sources in 5C7, the pulsar 5C7.256, is a Galactic object.

Apart from 5C2 and 5C5, there are as yet no other surveys at 408 MHz going deeper than 0.2 Jy which can be compared with 5C6 and 5C7, although deep surveys of area 0.026 sr made with the Molonglo telescope are being prepared for publication (Robertson 1977). Preliminary results from these, presented by Mills (1977) at IAU Symp. 74, show that between 0.09 and 0.2 Jy the source densities in these surveys are $\gtrsim 30$ per cent higher than in 5C2 and 5C5. This finding is consistent with the results from 5C6 and 5C7, and indicates that it is 5C2 and 5C5 which should be regarded as anomalous. The 5C3 and 5C4 areas (Pooley 1969; Willson 1970) also have slightly higher source densities than 5C2 and 5C5, but this could be attributed to the presence of M31 and the Coma cluster, both of which contribute sources to the catalogues.

Willis *et al.* (1977) compiled the source counts from surveys made with the Westerbork telescope at 610 MHz and found that dN/dS can be represented closely the curve

$$dN/dS = 912.06\, S^{(-2.39 - 0.101 \ln S)}$$

This curve, translated to 408 MHz by assuming that all sources have spectral index 0.8, is superimposed on the combined 5C5-7 source count in Fig. 7 and fits well, except at the lowest flux densites ($S_{408} < 30$ mJy) where the 'convergence' appears to be slightly more rapid at the lower frequency.

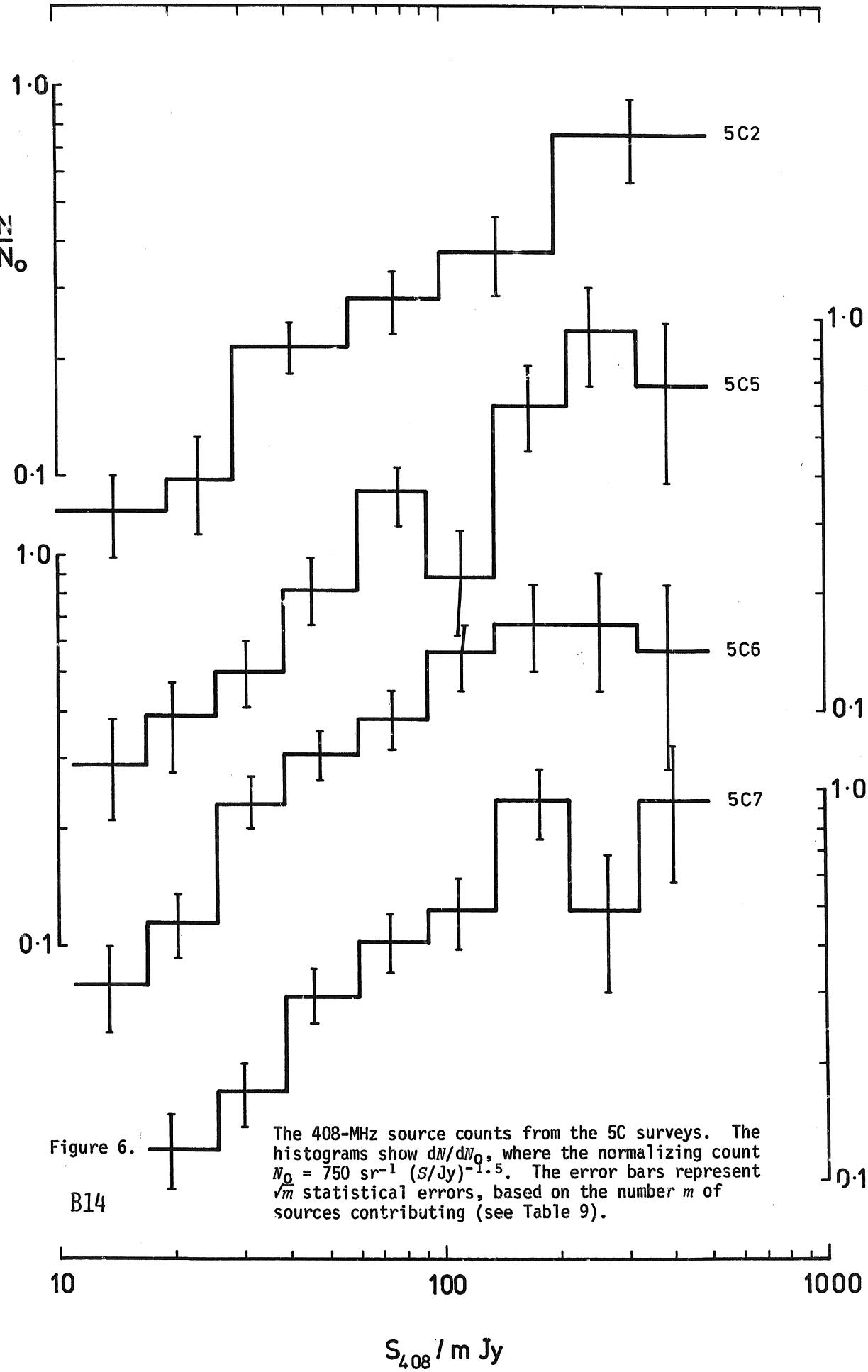

Figure 6.

The 408-MHz source counts from the 5C surveys. The histograms show dN/dN_0, where the normalizing count $N_0 = 750\ \mathrm{sr}^{-1}\ (S/\mathrm{Jy})^{-1.5}$. The error bars represent $\sqrt{m}$ statistical errors, based on the number m of sources contributing (see Table 9).

TABLE 9

Source Counts at 408 MHz

	5C6			5C7			5C5+6+7		
S	m	ΔN	$\Delta N/\Delta N_0$	m	ΔN	$\Delta N/\Delta N_0$	m	ΔN	$\Delta N/\Delta N_0$
11.0									
	15	0.245	0.0802				28	0.235	0.077
16.8									
	28	0.185	0.141	22	0.197	0.122	72	0.179	0.111
25.7									
	49	0.201	0.234	30	0.144	0.168	104	0.153	0.178
39.3									
	45	0.139	0.307	40	0.136	0.299	114	0.123	0.271
60.0									
	35	0.092	0.383	38	0.098	0.410	107	0.092	0.383
91.7									
	27	0.071	0.557	25	0.062	0.487	63	0.054	0.425
140.1									
	17	0.045	0.664	25	0.062	0.924	58	0.050	0.743
214.1									
	9	0.024	0.666	7	0.018	0.492	29	0.025	0.702
327.2									
	4	0.011	0.556	7	0.018	0.926	16	0.014	0.741
500.0									
Total	229			194			591		

S = flux density/mJy
m = number of sources detected
ΔN = corrected source density (10^5 sr^{-1})
ΔN_0 = expected source density if $N(S)$ = 750 sr^{-1} $(S/\mathrm{Jy})^{-1.5}$

TABLE 10

Source Counts at 1407 MHz

S	5C6 m	5C6 ΔN	5C6 $\Delta N/\Delta N_0$	5C7 m	5C7 ΔN	5C7 $\Delta N/\Delta N_0$	5C5+6+7 m	5C5+6+7 ΔN	5C5+6+7 $\Delta N/\Delta N_0$
2.2									
	10	0.893	0.081	8	0.626	0.057	30	0.959	0.087
5.7									
	17	0.576	0.218	23	0.814	0.308	54	0.608	0.230
14.8									
	7	0.214	0.338	7	0.213	0.337	19	0.183	0.290
38.5									
	3	0.092	0.607	1	0.030	0.199	7	0.068	0.450
100.0									
Total	37			39			110		

S = flux density/mJy
m = number of sources detected
ΔN = corrected source density (10^5 sr^{-1})
ΔN_0 = expected source density if $N(S)$ = 150 sr^{-1} $(S/\mathrm{Jy})^{-1.5}$

Figure 7 also shows the extension of dN/dN_o to higher flux densities derived from the Bologna B2 survey (Colla *et al.* 1973; 1.5 sr) and the all-sky catalogue of Robertson (1973; source counts from Mills, Davies & Robertson 1973).

The 5C and B2 data of Fig. 7 are displayed in integral form in Fig. 8. The purpose of this figure is to show the total source density, which is of interest for determining the confusion limit of a survey, whereas for statistical purposes the differential presentation is preferable. Figure 8 supersedes the integral source count by Pooley & Ryle (1968). It can be seen that the maximum source density in the 5C surveys is 10^5 sr^{-1}; for declinations greater than 25° this corresponds to > 40 beam areas per source in the centre of the field of view.

8.2 1407 MHz

The 1407-MHz source counts from 5C6 and 7 are shown in Table 10. Sources within the 0.20 contour of the envelope were counted if the uncorrected flux densities were greater than 2.0 mJy.

The counts from the three surveys were compared with the combined count by a χ^2-test similar to that used for 408 MHz. The result was $\chi^2 = 12.3$ (8 degrees of freedom) which is not significant at the 5 per cent level: there is thus no evidence for any difference between the three survey areas.

Because of the large uncertainties in the three counts, there is no point in plotting them individually. The combined count is shown in Fig. 9 with results from other surveys:

(a) $S > 2$ Jy: the BDFL catalogue (Bridle, Davis, Fomalont & Lequeux 1972);
(b) $0.55 < S < 2$ Jy: NRAO 300-ft GA survey (Davis, unpublished);
(c) $0.16 < S < 0.7$ Jy: NRAO 300-ft GB survey (Maslowski 1971, 1972a, 1972b, 1973);
(the above results are taken from the corrected compilation by Fomalont, Bridle & Davis 1974, and all are from 1400-MHz surveys);
(d) $0.01 < S < 0.11$ Jy: Cambridge Half-Mile telescope survey of 5C regions at 1421 MHz (Gillespie 1975);
(e) $0.002 < S < 0.2$ Jy: combined Westerbork 1415-MHz surveys (Willis *et al.* 1977); the curve plotted is the fitted curve of Willis *et al.*:

$$dN/dS = 310.72\ S^{(-2.59-0.106\ \ln S)}$$

Considering the uncertainty in the 5C counts, the agreement with (d) and (e) is fair; there is perhaps a deficiency of relatively bright sources, but not a serious one.

The major uncertainty remaining in the counts at low flux

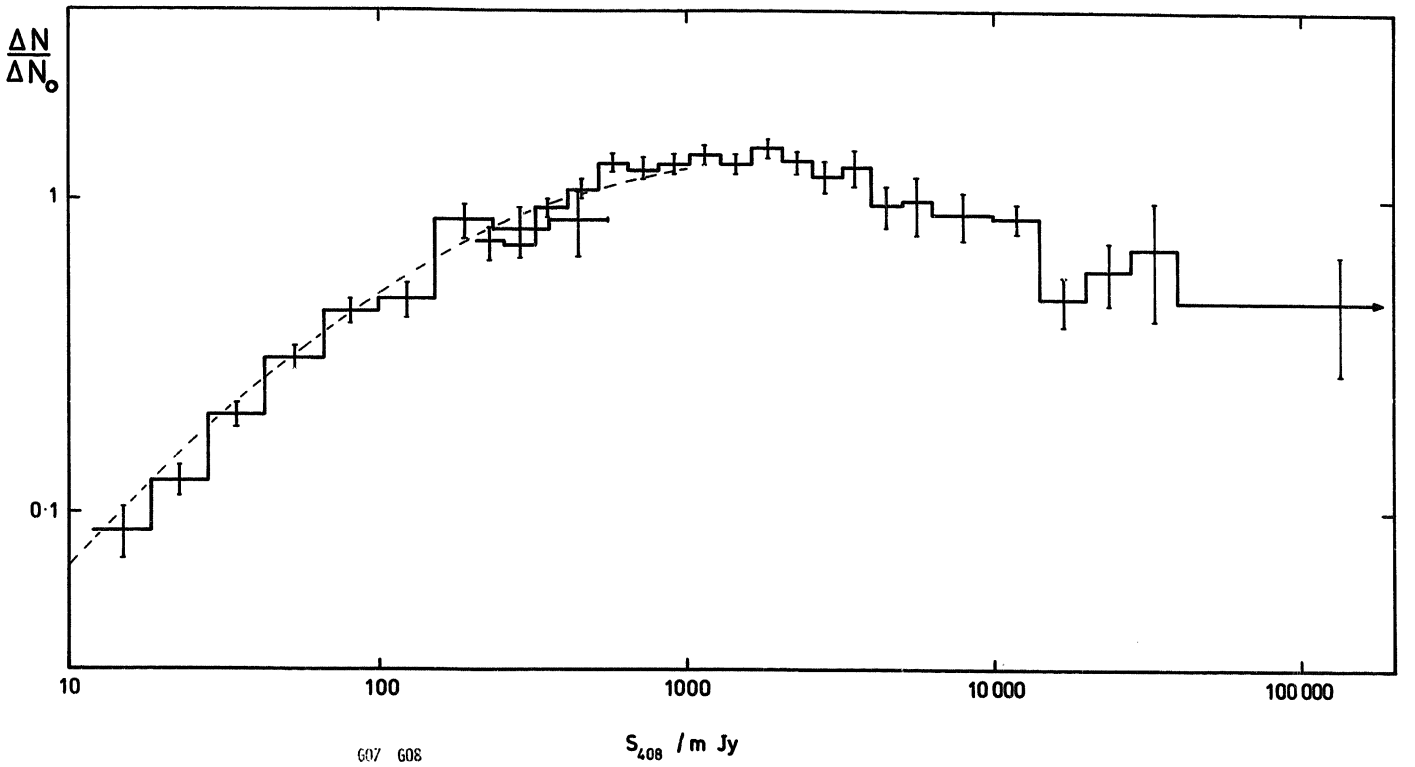

Figure 7. Source counts at 408 MHz. S > 10 Jy: all-sky catalogue (Mills *et al.* 1973); 10 Jy > S > 0.2 Jy: B2 survey (Colla *et al.* 1973); S < 0.5 Jy: 5C5-7 (Table 9). The smooth curve is scaled from the Westerbork 610-MHz counts of Willis *et al.* (1977). The normalization is N_0 = 750 sr^{-1} $(S/\mathrm{Jy})^{-1.5}$. Note that for this figure and for figure 8 the 5C flux densities have been increased by 9 per cent and the B2 flux densities have been increased by 6 per cent to conform to the scale of the all-sky catalogue (Wyllie 1969).

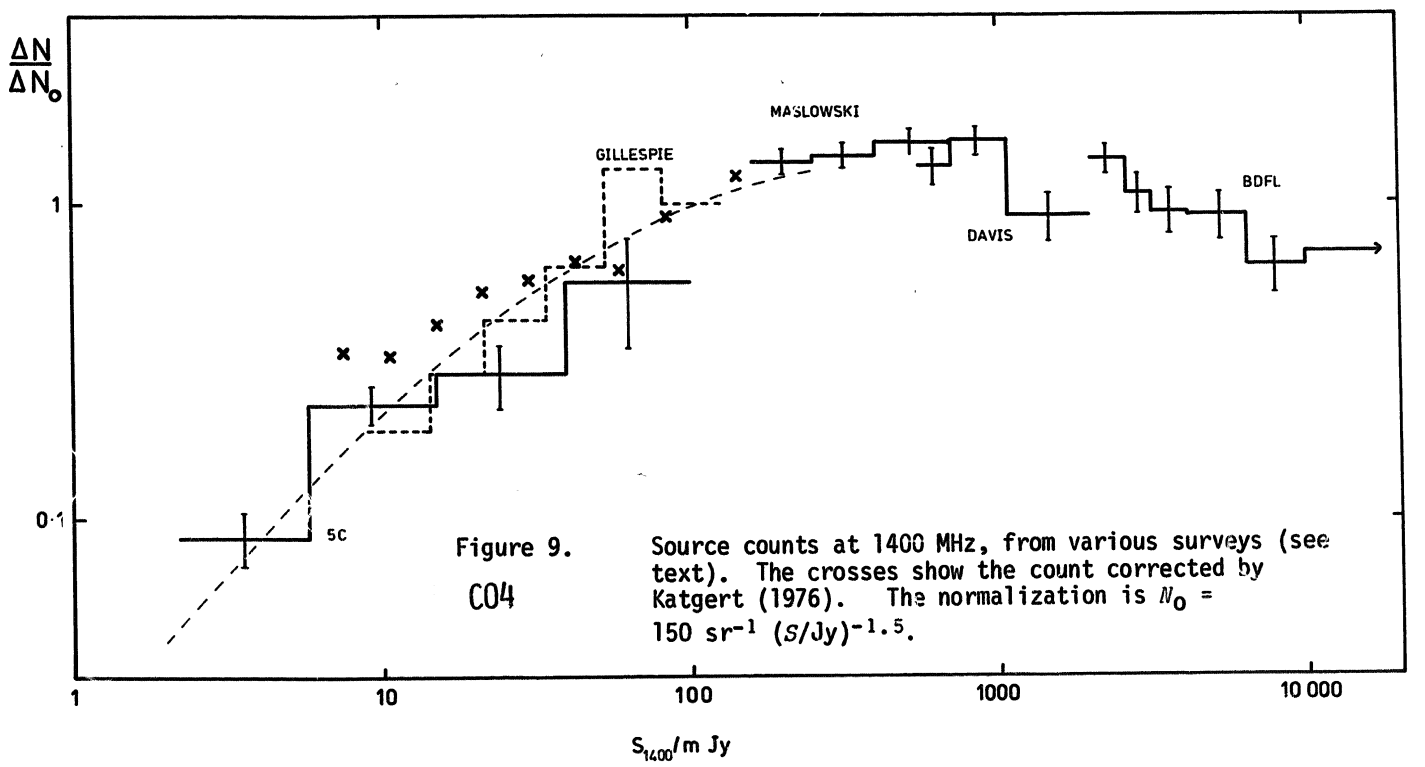

Figure 9. Source counts at 1400 MHz, from various surveys (see text). The crosses show the count corrected by Katgert (1976). The normalization is N_0 = 150 sr^{-1} $(S/\mathrm{Jy})^{-1.5}$.

C04

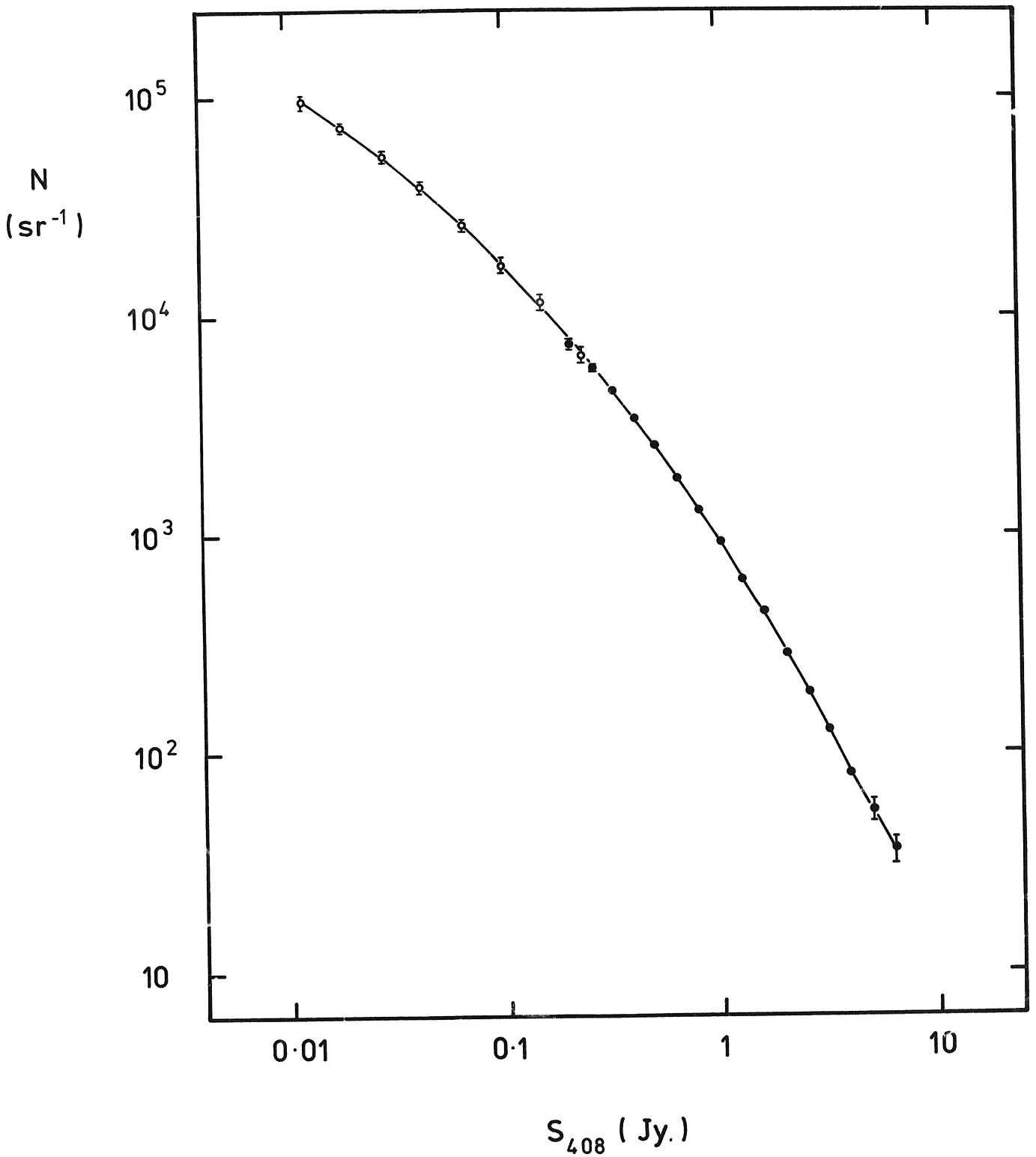

Figure 8. Integral $N(S)$ at 408 MHz from the B2 survey (filled circles) and 5C5-7 (open circles); Wyllie scale. Some of the error bars have been omitted.

C05

densities is the magnitude of the systematic underestimation of dN/dS due to resolution. The Westerbork curve (e) has not been corrected for this effect, and it is anticipated that the correction will cause a significant increase in dN/dS. The only survey that has so far been corrected is that of Katgert (1975, 1976); his corrected source count covers the range $6.25 < S_{1415} < 200$ mJy, and below $\simeq 30$ mJy his dN/dS is greater than that of (e) by a factor $\simeq 1.4$, which is fully accounted for by his 'resolution correction'.

It is unlikely, however, that the 5C counts can be made consistent with Katgert's by applying a similar resolution correction; because the noise level in the 5C surveys is smaller, the correction (at a given flux density level) would also be smaller. Although the resolution effect in the 5C surveys has not been analysed so carefully as Katgert has done, the use of low-resolution maps has ensured that the catalogues are complete for sources smaller than 30 arcsec and stronger than 3 mJy. From Katgert's model of the angular size distribution, the fraction of sources larger than 30 arcsec is estimated to be < 20 per cent, so that the required correction to the source counts at 3 mJy is less than 20 per cent, and smaller at higher flux densities. This is much less than the correction that would be required to raise the 5C count to meet Katgert's. It can be concluded that either the region of Katgert's survey has an anomalously high source density at 1415 MHz, or that he has overcorrected the source counts.

9 Spectral index distributions

9.1 SOURCES SELECTED AT 1407 MHz

Many of the sources detected at 1407 MHz have no 408 MHz flux density estimates owing to the difference in sensitivity between the two frequencies. In order to derive spectral indices for a complete sample of sources selected at 1407 MHz, estimates of, or upper limits to, S_{408} for these sources were derived by inspection of the 408-MHz contour maps. Even if these sources are included, the sample is not complete above a fixed limiting flux density, because of the variation of 1407-MHz sensitivity across the field of view; but, because the sensitivity at 408 MHz is almost uniform over the region surveyed at 1407 MHz, the spectral index distribution derived from the sample is unbiased, and only differs significantly from the true distribution $g_S^{1407}[\alpha(408,1407)]$* if there is a strong dependence of g_S^{1407} on flux density S. A better estimate of g_S^{1407} can be derived by weighting each source according to the area over which it could have been observed (as

---

*$g_S^{\nu}[\alpha(\nu_1,\nu_2)]$ is the distribution of two-point spectral index α (between frequencies ν_1 and ν_2) in a sample of sources with flux density greater than S at frequency ν.

has been done by Katgert & Spinrad 1974), but the distribution is then dominated by a small number of weak sources which have large weights, and it is difficult to assess statistically; this procedure is only necessary if a significant proportion of the sources in the sample is not detected at one of the two frequencies.

Spectral index distributions g^{1407} [α(408,1407)] derived from 5C5, 6 and 7 are shown in Fig. 10. Each distribution includes all the sources detected at 1407 MHz within the 15 per cent contour of the envelope, and each source has been given equal weight. Some characteristic statistics of the spectral-index distributions are listed in Table 11. It can be seen that the three distributions are very similar. The median of the 5C6 distribution is lower than those of the other two, but this difference is within the uncertainty of the calibration of the flux-density scales.

The sample of sources with 10 mJy < S_{1407} < 200 mJy from 5C5, 6 and 7 is compared in Fig. 11 and Table 11 with the similar sample compiled by Willson (1972a) from 5C2, 3 and 4. It can be seen that the median spectral index and fraction of sources with α < 0.5 are very similar in the two samples. There is no evidence for any anisotropy in the spectral-index distribution. Figure 11 also includes the estimate of $g^{1407}_{0.01}$ [α(408,1407)] derived from sources in the flux-density range 10 mJy < S_{1407} < 200 mJy from all six surveys (5C2-7). This distribution includes 98 sources.

Two other observations of g^{1400}_{S} (α) are available for comparison with the 5C results, and the statistics of these observations are included in Table 11.

(a) The Half-Mile telescope surveys (Gillespie 1975). The spectral-index distribution from these observations of the 5C1-5 areas is $g^{1421}_{0.01}$ [α(408,1421)]. Note that because some of the sources are the same as in the 5C2-7 sample, the distributions are not strictly independent.

(b) The Westerbork surveys : $g^{1415}_{0.02}$ [α(610,1415)]. The first Westerbork 610-MHz survey (Katgert & Spinrad 1974) produced an unexpectedly broad spectral-index distribution, including a much larger proportion of flat spectra than the 5C and Half-Mile samples. In a sample of 36 sources with S_{1415} > 0.01 Jy, the mean α(610,1415) was 0.52, with a dispersion 0.39. Subsequent Westerbork surveys have shown that this first estimate was atypical; in a larger sample of 174 sources, the mean is 0.64 ± 0.03 (Table 11; Katgert *et al.* 1977).

Differences in the flux-density scales will cause the three g(α) (5C, Half-Mile and Westerbork) to be shifted relative to one another. The 5C and Half-Mile surveys are referred to the KPW

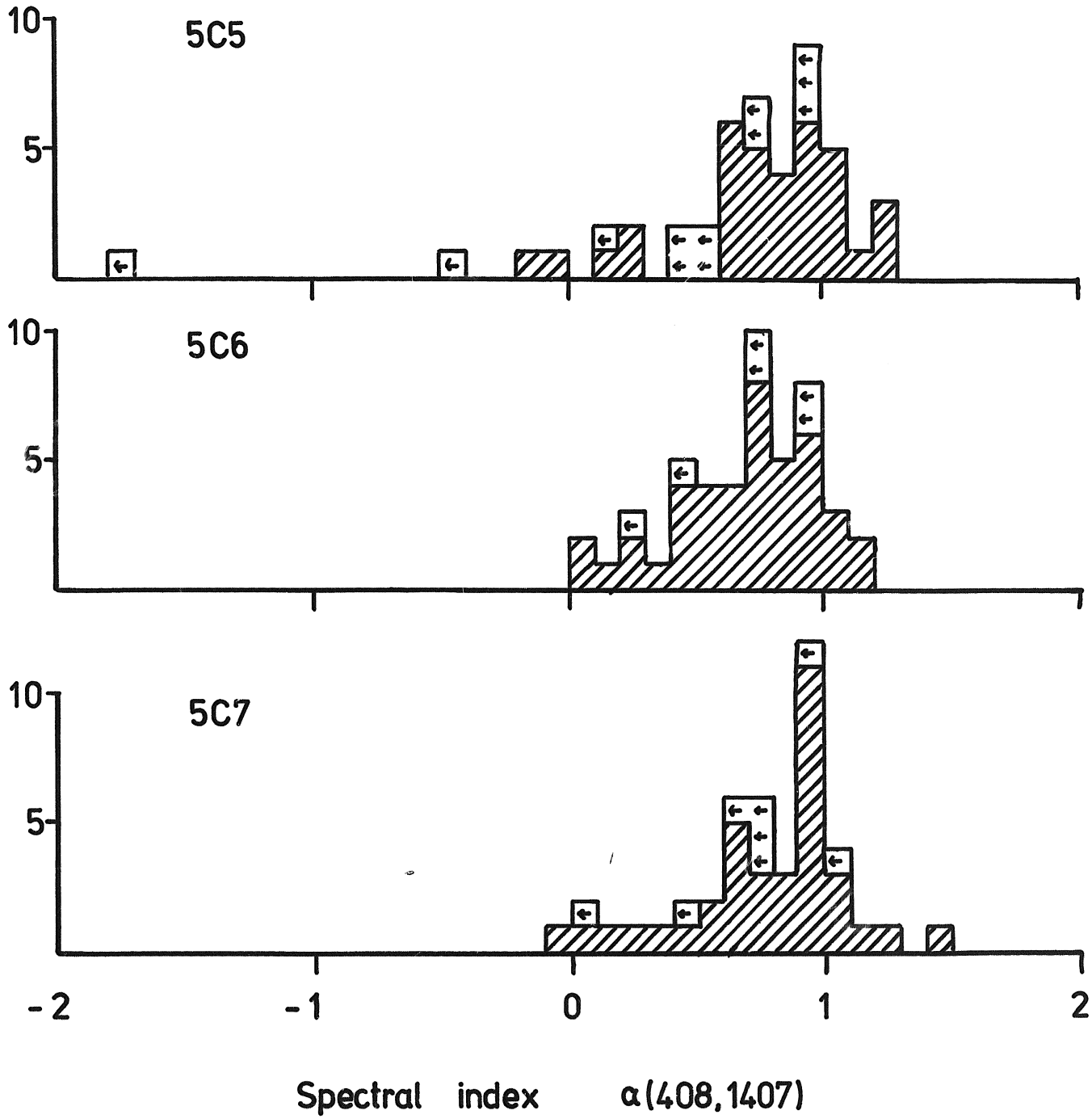

Figure 10. Spectral-index distributions of sources detected at 1407 MHz in 5C5, 5C6 and 5C7; arrows indicate upper limits.

C08

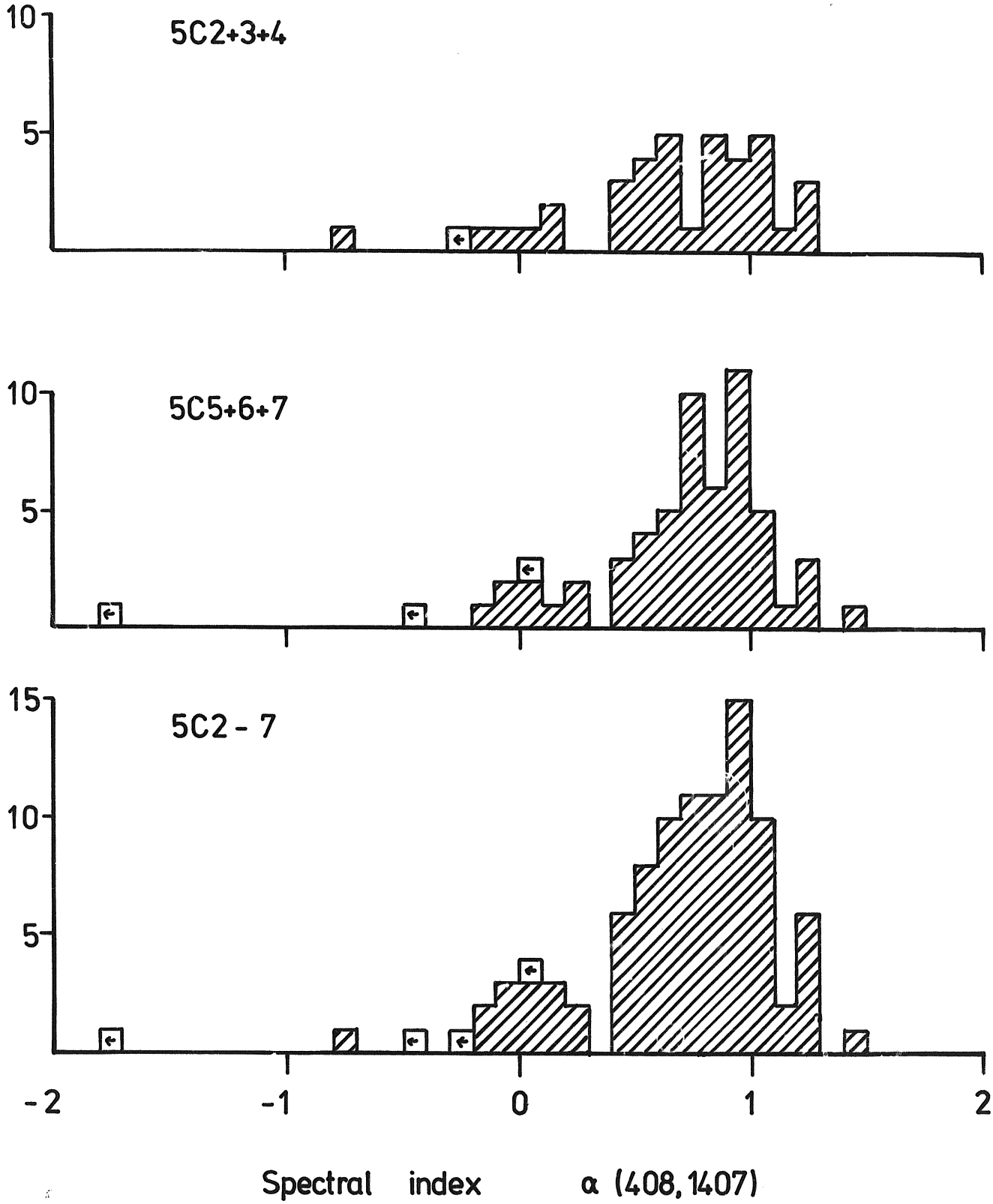

Figure 11. Spectral-index distributions of sources with 10 mJy < S_{1407} < 200 mJy detected in 5C2+3+4 (Willson 1972a) and in 5C5+6+7. The bottom histogram is the sum of the other two.

C09

TABLE 11

Statistics of spectral index distributions at 1400 MHz

	Number of sources	Mean	Median	Fraction $\alpha < 0.5$	Mean and standard devn. (excluding $\alpha < 0.3$)	
5C5: all sources detected at 1407 MHz	47	0.67±0.07	0.79	0.21±0.06	0.85±0.03	0.20
5C6: all sources detected at 1407 MHz	48	0.69±0.04	0.74	0.25±0.06	0.76±0.03	0.20
5C7: all sources detected at 1407 MHz	44	0.75±0.05	0.80	0.18±0.06	0.83±0.04	0.22
Samples with $10 < S_{1400} < 200$ mJy:						
5C2, 3 and 4 (Willson 1972a)	38	0.72±0.06	0.77	0.26±0.07	0.83±0.04	0.25
5C5, 6 and 7	60	0.66±0.06	0.77	0.23±0.05	0.84±0.03	0.22
5C2-7	98	0.68±0.04	0.77	0.24±0.04	0.84±0.03	0.23
Comparison samples:						
Westerbork (Katgert *et al.* 1977)	174*	0.64±0.03		0.25±0.04		
Half-Mile (Gillespie 1975)	140	0.71±0.03	0.80	0.21±0.04	0.81±0.03	0.20
BDFL/B2 (2 Jy) (Katgert *et al.* 1977)	50	0.61±0.05		0.25±0.07		

Notes:

* The Westerbork sample contains a further 9 sources for which S_{610} is not available.

The statistics have been calculated by including both upper limits and true estimates with equal weight.

flux-density scale at both 408 MHz and 1400 MHz, so that no differences are expected; and Katgert *et al.* (1977) suggest that a difference in the 1400-MHz flux-density scales can account for a difference of 0.08 in mean spectral index between the Half-Mile and Westerbork surveys. With this correction, there is no evidence for any difference in mean or median spectral-index between the three samples. The dispersions of each distribution will be different if the uncertainties in the individual spectral-index measurements are different, but because the sources detected in all the surveys have similar signal-to-noise ratios, these differences should be small. The typical rms uncertainty in a single estimate of α from the new 5C surveys is about 0.1; in the older surveys it is larger, $\approx$ 0.17 (Willson 1972a), on account of the higher 1407-MHz noise level, and the dispersion of $g(\alpha)$ is correspondingly larger. The intrinsic rms dispersion of $g(\alpha)$ is $\approx$ 0.16.

The 5C surveys confirm the spectral-index distributions found in the other surveys, and they thus confirm the remarkable fact that there is no apparent variation of the distribution g_S^{1400} [α(408,1400)] with flux density. Making allowance for the different flux-density scales, Katgert *et al.* show that the difference in mean spectral index between 2 Jy and 20 mJy is 0.01 $\pm$ 0.09. This absence of change in mean spectral index contrasts with the conclusion of Willson (1972a) that the median spectral index is larger in the 5C2,3,4 sample than at high flux densities, the new result being due to improvements in the determination of the spectral-index distributions at high flux densities. The correlation of extended sources with those having steep spectra, noticed by Willson and discussed further by Fanaroff & Longair (1972), is not present in the results of 5C5, 6 and 7.

9.2 SOURCES SELECTED AT 408 MHz

It is possible to derive spectral-index distributions for sources selected at 408 MHz instead of 1407 MHz; but because almost all the sources are the same ones as those in the 1407-MHz samples, the results are not independent - there is certainly no independent information on the differences between the various surveys. For this reason, and because better estimates of g_S^{408} (α) are available, only one of the 5C surveys will be considered. The spectral index distribution of the sample of 37 sources with S_{408} > 10 mJy from 5C6 includes one lower limit. The median is 0.80 and the fraction with α < 0.5 is 0.14 $\pm$ 0.06. The fraction of flat-spectrum sources is significantly less than in the 1407-MHz samples, and the median is slightly greater. The distribution as a whole agrees well with that derived by Katgert (1976) from a sample of 137 5C2 sources. Taking into account the differences in the flux-density scales between different surveys, Katgert showed that there is an (insignificant) increase

in the mean of $g_S^{408}(\alpha)$ by 0.09 ± 0.07 when S is decreased from 5.5 Jy to 0.06 Jy. This result and the results of Pauliny-Toth *et al.* (1972) for S_{408} = 2 Jy and 0.5 Jy [α(408,5000)] indicate that there is no evidence for a variation of mean spectral index with flux density below 5.5 Jy; it appears, though, that the mean spectral index is greater for S > 10 Jy when sources with complex, flat or inverted spectra are excluded (Murdoch 1976). In comparisons of this kind, great care must be taken to ensure that the data are uniform, especially with regard to their flux-density scales. The present data are certainly not uniform, as different definitions of spectral index have been used for the different surveys, so no firm conclusions can be drawn until further work is done.

10 Clustering

Webster & Pearson (1977) examined the distribution of the 408-MHz sources in 5C5, 5C6 and 5C7 by the method of Power Spectrum Analysis. They found no evidence for clustering of the sources on any scale $\lesssim$ 1 degree.

11 Conclusions

11.1 FLUX DENSITY

The new 5C surveys have greatly improved the definition of the 408-MHz source counts between 10 mJy and 200 mJy. The 'convergence' of the source counts at low frequencies is now very well defined. The 5C surveys are in excellent agreement both with each other and with other surveys. The source counts at 1407 MHz supplement, and generally confirm, the results of the more extensive Westerbork surveys between 2 mJy and 200 mJy.

11.2 SPECTRUM

The low-frequency spectral-index distribution of sources selected at 1407 MHz from the 5C surveys could be improved by more extensive observations, but it already appears that there is no substantial change in its form for a change of flux density by a factor of 1000. This result is of cosmological interest, and deserves further investigation, particularly by additional observation at intermediate flux densities (between 0.2 and 1 Jy). The sample at low flux densities cannot easily be enlarged by additional 5C surveys alone, owing to the small size of the 1407-MHz field of view; a better strategy would be to make 408-MHz (5C) surveys of areas that have already been covered by deep 1400-MHz surveys at Westerbork (or elsewhere), and similarly to re-observe at Westerbork the full fields of 5C5, 6 and 7 at 1400 MHz (as Katgert has done for 5C2).

11.3 ANGULAR STRUCTURE

There is little information on angular sizes available from the 5C surveys. The new surveys have however confirmed that 30 per cent of sources with $S > 3$ mJy have angular size > 10 arcsec, and that a small proportion have angular size > 80 arcsec. There may be sufficient information in 5C5, 6 and 7 to make it worthwhile now to repeat the analysis of Longair & Pooley (1969) but the difficulty of detecting sources larger than 3 arcmin could prevent firm conclusions being drawn.

11.4 OPTICAL IDENTIFICATION

The identification of 5C6 and 5C7 sources described in Section 6 is only preliminary, but the importance of further identification work has been established by Wall, Pearson & Longair (1977). 5C6 and 5C7 are ideal for careful statistical identification as we have greater faith in the accuracy of their positions than for the earlier surveys, and indeed Schmidt plates of the 5C6 and 5C7 areas have already been taken by Dr M.V. Penston. The accuracy of 5C5 has yet to be confirmed, and a number of the brightest 5C5 sources are presently being observed at 2.7-GHz with the 5-km telescope to determine what corrections to the 5C5 positions may be necessary; this programme will also enable us to investigate the structure of a sample of relatively weak sources.

11.5 ISOTROPY

None of the results of the 5C6 and 5C7 surveys has provided any evidence for anisotropy of faint radio sources. The source counts and spectral-index distributions of the surveys agree well, and there is no suggestion that the radio sources are not randomly and uniformly distributed on the sky.

Acknowledgments

We thank the many members of the Mullard Radio Astronomy Observatory who assisted us with these observations and their interpretation, especially Dr Guy Pooley. TJP thanks the Science Research Council for a research studentship, and AJK thanks the British Council for a scholarship. We are very grateful to Mrs. L. Cooper and Mrs. M. Jones for typing the paper so carefully.

References

Bridle, A.H., Davis, M.M., Fomalont, E.B. & Lequeux, J., 1972. *Astr. J.*, 77, 405.

Colla, G., Fanti, C., Fanti, R., Ficarra, A., Formiggini, L., Gandolfi, E., Grueff, G., Lari, C., Padrielli, L., Roffi, G., Tomasi, P. & Vigotti, M., 1970. *Astr. Astrophys. Suppl.*, 1, 281.

Colla, G., Fanti, C., Fanti, R., Ficarra, A., Formiggini, L., Gandolfi, E., Lari, C., Marano, B., Padrielli, L. & Tomasi, P., 1972. *Astr. Astrophys. Suppl.*, 7, 1.

Colla, G., Fanti, C., Fanti, R., Ficarra, A., Formiggini, L., Gandolfi, E., Gioia, I., Lari, C., Marano, B., Padrielli, L. & Tomasi, P., 1973. *Astr. Astrophys. Suppl.*, 11, 291.

Condon, J.J. & Jauncey, D.L., 1973. *Astrophys. J.*, 184, L33.

Davis, M.M., 1971. *Astr. J.*, 76, 980.

de Ruiter, H.R., Willis, A.G. & Arp, H.C., 1977. *Astr. Astrophys. Suppl.*, 28, 211.

Fanaroff, B.L. & Longair, M.S., 1972. *Mon. Not. R. astr. Soc.*, 159, 119.

Fanti, R., Ficarra, A., Formiggini, L., Gioia, I. & Padrielli, L., 1974. *Astr. Astrophys.*, 32, 155.

Fanti, C., Fanti, R., Ficarra, A., Formiggini, L., Giovannini, C., Lari, C. & Padrielli, L., 1975. *Astr. Astrophys. Suppl.*, 19, 143.

Fomalont, E.B., Bridle, A.H. & Davis, M.M., 1974. *Astr. Astrophys.*, 36, 273.

Gearhart, M.R., Kraus, J.D. & Andrew, B.H., 1976. *Astrophys. J. Suppl.*, 30, 337.

Ghigo, F.D. & Owen, F.N., 1973. *Astr. J.*, 78, 848.

Gillespie, A.R., 1974. *Surveys of faint radio sources at 1420 MHz*, Ph.D. dissertation, University of Cambridge.

Gillespie, A.R., 1975. *Mon. Not. R. astr. Soc.*, 170, 541.

Gillespie, A.R., 1977. *Mon. Not. R. astr. Soc.*, (in press).

Grueff, G. & Vigotti, M., 1973. *Astr. Astrophys. Suppl.*, 11, 41.

Grueff, G. & Vigotti, M., 1975. *Astr. Astrophys. Suppl.*, 19, 117.

Hazard, C., Gulkis, S. & Sutton, J., 1968. *Astrophys. J.*, 154, 413.

Högbom, J.A., 1974. *Astr. Astrophys. Suppl.*, 15, 417.

Katgert, J.K. & Spinrad, H., 1974. *Astr. Astrophys.*, 35, 393.

Katgert, P., 1975. *Astr. Astrophys.*, 38, 87.

Katgert, P., 1976. *Astr. Astrophys.*, 49, 221.

Katgert, P., Padrielli, L., Katgert, J.K. & Willis, A.G., 1977. 'Spectral index distributions of extragalactic radio sources', in IAU Symp. 74, *Radio astronomy and cosmology*, ed. D. Jauncey.

Kellermann, K.I., Pauliny-Toth, I.I.K. & Williams, P.J.S., 1969. *Astrophys. J.*, 157, 1.

Longair, M.S., 1974. 'The counts of radio sources', in IAU Symp. 63, *Confrontation of cosmological theories with observational data*, ed. M.S. Longair.

Longair, M.S. & Pooley, G.G., 1969. *Mon. Not. R. astr. Soc.*, 145, 121.

Manchester, R.N. & Taylor, J.H., 1972. *Astrophys. Lett.*, 10, 67.

Maslowski, J., 1971. *Astr. Astrophys.*, 14, 215.

Maslowski, J., 1972a. *Astr. Astrophys.*, 16, 197.

Maslowski, J., 1972b. *Acta Astronomica*, 22, 227.

Maslowski, J., 1973. *Astr. Astrophys.*, 26, 343.

Mills, B.Y., 1977. 'The Molonglo radio source surveys at 408 MHz', in IAU Symp. 74, *Radio astronomy and cosmology*, ed. D. Jauncey.

Mills, B.Y., Davies, I.M. & Robertson, J.G., 1973. *Austr. J. Phys.*, 26, 417.

Murdoch, H.S., 1976. *Mon. Not. R. astr. Soc.*, 177, 441.

Neville, A.C., Windram, M.D. & Kenderdine, S., 1969. *Observatory*, 89, 186.

Notni, P., Oleak, H. & Richter, G.M., 1971. *Astr. Nachr.*, 293, 221.

Parkes, A.G. & Penston, M.V., 1973. *Mon. Not. R. astr. Soc.*, 162, 117.

DOI

Pauliny-Toth, I.I.K., Kellermann, K.I. & Davis, M.M., 1972. 'Number counts and spectral distribution of radio sources at centimeter wavelengths', in IAU Symp. 44, *External galaxies and quasi-stellar objects*, ed. D.S. Evans.

Pauliny-Toth, I.I.K., Witzel, A. & Preuss, E., 1974. *Astr. Astrophys.*, 35, 421.

Pearson, T.J., 1975. *Mon. Not. R. astr. Soc.*, 171, 475.

Pilkington, J.D.H. & Scott, P.F., 1965. *Mem. R. astr. Soc.*, 69, 183.

Pooley, G.G., 1969. *Mon. Not. R. astr. Soc.*, 144, 101.

Pooley, G.G. & Kenderdine, S., 1968. *Mon. Not. R. astr. Soc.*, 139, 529.

Pooley, G.G. & Ryle, M., 1968. *Mon. Not. R. astr. Soc.*, 139, 515.

Reichley, P.E., Downs, G.S. & Morris, G.A., 1970. *Astrophys. J.*, 159, L35.

Richter, G.A., Richter, G.M., Richter, L. & Richter, N.B., 1974. *Astr. Nachr.*, 295, 19.

Robertson, J.G., 1973. *Austr. J. Phys.*, 26, 403.

Robertson, J.G., 1977. *Austr. J. Phys.*, 30, 241.

Ryle, M., 1972. *Nature*, 239, 435.

Shimmins, A.J. & Day, G.A., 1968. *Austr. J. Phys.*, 21, 377.

Spencer, J.M. & Burke, B.F., 1975. *Astrophys. J.*, 199, 611.

Thompson, A.R. & Bracewell, R.N., 1974. *Astr. J.*, 79, 11.

van der Kruit, P.C. & Katgert, P., 1972. *Astrophys. Lett.*, 11, 181.

Vorontsov-Vel'yaminov, B.A. & Arkhipova, V.P., 1964. *Morphological catalogue of galaxies - II.* Moscow University Press.

Wall, J.V., Pearson, T.J., & Longair, M.S., 1977. 'Interpretation of source counts and redshift data in evolutionary universes' in IAU Symp. 74, *Radio astronomy and cosmology*, ed. D. Jauncey.

Warwick, R.S., 1977. *Mon. Not. R. astr. Soc.*, 179, 1.

Webster, A. & Pearson, T.J., 1977. *Mon. Not. R. astr. Soc.*, 179, 517.

Weiler, K.W., Goss, W.M. & Schwarz, U.J., 1974. *Astr. Astrophys.*, 35, 473.

Willis, A.G., Oosterbaan, C.E. & de Ruiter, H.R., 1976. *Astr. Astrophys. Suppl.*, 25, 453.

Willis, A.G., Oosterbaan, C.E., Le Poole, R.S., de Ruiter, H.R., Strom, R.G., Valentijn, E.A., Katgert, P. & Katgert-Merkelijn, J., 1977. 'Westerbork surveys of radio sources at 610 MHz and 1415 MHz', in IAU Symp. 74, *Radio astronomy and cosmology*, ed. D. Jauncey.

Wills, D. & Wills, B.J., 1976. *Astrophys. J. Suppl.*, 31, 143.

Willson, M.A.G., 1970. *Mon. Not. R. astr. Soc.*, 151, 1.

Willson, M.A.G., 1972a. *Mon. Not. R. astr. Soc.*, 155, 385.

Willson, M.A.G., 1972b. *Mon. Not. R. astr. Soc.*, 156, 7.

Wyllie, D.V., 1969. *Mon. Not. R. astr. Soc.*, 142, 229.

TABLE 2 The 5C6 Survey

[1]		[2]	[3]	[4]	[5]	[6]	[7]	[8]	[9]	[10]	[11]	[12]
1	02	3 1.4	32 48 4	8	320	*	0.03					18m red object 5"f; sl conf by ring
2		3 20.6	33 22 45	3	1237	*	0.02					19m red object; B2 0203+33
3		3 46.8	32 7 54	3	456	*	0.07					-
4		4 0.7	32 47 10	1	2322	*	0.06					19m blue star 10"p; 4C 32.10, B2 0204+32
5		4 14.0	33 22 24	5	500	*	0.04					19m blue star; GC 0204+33
6	02	4 20.6	31 59 17	6	129	*	0.10					-
7		4 25.7	32 23 31	7	115	*	0.10					18m star
8		4 39.9	31 37 51	1	1300	350	0.11					19m objects 10"Np and 10"f; B2 0204+31
9		4 50.5	32 52 51	5	175	*	0.09					19m star 20"f, 20m red object 20"N
10		5 3.1	31 53 6	5	105	26	0.14					-
11	02	5 12.7	31 22 40	5	129	33	0.13					conf by grating ring
12		6 0.3	31 52 36	2	210	31	0.22					B2 0205+31
13		6 5.1	32 23 53	5	74	15	0.21					sl extended pa 45
14		6 5.9	31 31 58	7	56	13	0.21					17m blue galaxy 10"N
15		6 6.0	31 14 13	4	128	24	0.18					20m blue object 15"p
16	02	6 9.5	32 44 11	6	74	17	0.18					16m star 15"S, 19m object 15"p
17		6 22.2	34 14 28	8	460	*	0.02					B2 0206+34
18		6 23.8	32 26 38	3	128	19	0.23					19m star 20"p
19		6 30.2	33 40 11	1	1421	*	0.07					B2 0206+33, conf by grating ring
20		6 47.6	31 9 3	2	161	24	0.22					20m object 10-15"S; sl extended pa 45
21	02	6 55.0	31 57 49	6	44	8	0.30					19m red object 20"Nf
22		7 15.1	32 0 55	3	78	9	0.34					-
23		7 15.9	30 55 55	2	166	25	0.22					sl extended ?
24		7 20.4	32 35 25	1	710	71	0.30					18m star 15"Sp; B2 0207+32
25		7 27.1	33 56 35	3	543	*	0.06					B2 0207+33
26	02	7 26.4	32 25 5	6	42	7	0.33					18m star 10"S; conf by sidelobe of 24
27		7 50.5	31 32 21	7	32	6	0.37					-
28		8 3.3	31 3 34	5	56	9	0.31					15m galaxy (60"x15")
29		8 9.1	32 42 38	1	309	26	0.36					B2 0208+32A
30		8 9.2	33 38 24	6	102	27	0.14					-
31	02	8 20.3	31 57 31	4	40	5	0.46					19-20m red object 10"N, 17-18m star 15"Sf
32		8 29.2	31 7 50	6	40	7	0.36					18-19m stars 10"N and 15"Nf
33		8 36.7	33 34 16	2	343	60	0.17					B2 0208+33, sl extended pa 270
34		8 39.0	31 21 30	1	245	18	0.43					19-20m blue object, 19m blue object 5"pa; B2 0208+31
35		8 43.6	33 45 14	e	83	24	0.13					No clear candidate; component 2' Nf
36	02	8 43.7	32 50 11	4	54	7	0.39					-
37		8 47.9	31 51 7	4	39	5	0.52					several 19m red objects; extended pa 90
38		8 52.1	31 0 29	6	35	6	0.36					20m object 10"p; conf by sidelobe of 40
39		8 53.9	32 14 48	1	272	16	0.52					B2 0208+32B
40		8 55.7	30 49 17	7	38	8	0.32					19m red object; sl extended pa 45

[1]	[2]	[3]	[4]	[5]	[6]	[7]	[8]	[9]	[10]	[11]	[12]
41	02	8 55.8	31 40 4	6	27	4	0.51				-
42		9 1.8	31 2 17	2	128	11	0.39				-
43		9 4.8	33 48 2	2	469	104	0.14				B2 0209+33
44		9 6.0	30 21 3	8	53	13	0.20				-
45		9 8.0	32 6 12	4	40	4	0.56				20m object; ? sl extended pa 270
46	02	9 21.5	30 25 19	3	146	21	0.23				-
47		9 26.2	32 12 21	3	41	4	0.59				-
48		9 28.0	31 14 18	5	31	5	0.49				-
49		9 35.3	30 50 19	7	29	6	0.37				-
50		9 36.3	30 31 33	6	49	9	0.27				20m red object, and several others within 15"
51	02	9 44.2	33 28 9	5	66	11	0.26				conf by sidelobe of 55; extended ?
52		9 46.4	31 45 12	8	17	3	0.63				20m object 10"Np
53		9 53.4	33 1 54	2	100	9	0.43				19m object 15"N
54		9 55.8	32 15 32	6	21	3	0.65				-
55		9 56.9	33 27 30	3	103	13	0.28				-
56	02	10 4.6	31 38 55	6	20	3	0.65				-
57		10 8.5	32 38 42	6	24	4	0.59				15-16m star 10"Sf; conf by sidelobes
58		10 14.1	31 34 6	3	43	4	0.65				extended pa 150
59		10 18.8	30 50 16	6	34	5	0.43				19m object 10-15"S
60		10 19.8	32 3 51	6	18	3	0.71				-
61	02	10 26.4	31 49 46	4	28	3	0.72				20-21m red object
62		10 29.6	32 53 56	1	402	23	0.53				20m object; B2 0210+32
63		10 30.1	34 4 19	2	439	120	0.11				B2 0210+34
64		10 33.3	32 47 21	7	19	4	0.58				conf by sidelobes of 62 and 69
65		10 34.8	30 46 45	4	55	6	0.43				19-20m object
66	02	10 37.8	31 30 38	2	53	4	0.68				19m object 15"p
67		10 41.1	33 53 45	3	158	31	0.17				19-20m red object 10"Np
68		10 42.4	31 45 8	1	183	8	0.74				extended pa 270
69		10 43.2	32 46 4	2	71	5	0.60				18m blue object 15-20"N; conf by sidelobe of 62
70		10 47.4	32 31 8	5	24	3	0.69				conf by sidelobe of 78
71	02	10 54.7	32 12 10	4	28	3	0.76				18-19m blue star 10"S
72		11 0.0	31 38 53	4	30	3	0.75				two faint objects
73		11 1.0	32 26 1	3	43	3	0.74				18-19m star 15"f; ? sl extended pa 320
74		11 3.2	30 22 5	2	170	19	0.30				17m star 15"Sp, 19m red object 10"Nf; Part of B2 0211+30A
75		11 6.3	30 12 15	2	263	34	0.24				Part of B2 0211+30A
76	02	11 6.6	31 4 16	2	69	5	0.58				19m object 15"N
77		11 6.9	31 49 11	5	19	3	0.79				20m object 5"N
78		11 8.26	32 36 7.7	0.3	563	24	0.70	+			see 88; B2 0211+32A; extended (see text) r=1.4
79		11 10.0	32 52 2	5	30	4	0.60				19m red object 10"S; conf by sidelobes
80		11 10.1	30 8 14	6	60	13	0.22				conf by sidelobe of 75

[1]	[2]	[3]	[4]	[5]	[6]	[7]	[8]	[9]	[10]	[11]	[12]
81a	02 11 10.56	31 52 58.1	2.1	63	4	0.80	12.1	3.0	0.17		several optical objects; r=0.97 (a+b)
b	11 12.98	31 52 41.8	1.9				12.5	2.9	0.17		See map
82	11 11.0	33 4 46	2	74	6	0.51					19m blue object 10"p; extended? confused by 84
83	11 11.5	30 39 50	1	677	49	0.42					19m object 10"Nf, faint red object 10"Sp; B2 0211+30B
84	11 13.9	33 7 53	1	165	11	0.49					20m blue object; confused by 82
85	11 17.4	32 57 13	7	20	4	0.58					18m red object 10"f, 20m blue object 10"Sp
86	02 11 22.0	30 11 3	3	132	18	0.24					19m red object 5"p and several others
87	11 26.7	30 43 30	3	58	6	0.46					conf by sidelobe of 83
88a	11 26.97	32 37 51.6	0.3	713	30	0.72	+				19m galaxy between 78 and 88; B2
b	11 30.18	32 38 10.4	0.3								0211+32B; extended (see 78)
89	11 30.2	31 11 48	3	43	4	0.66					-
90	11 32.0	31 32 19	8	13	3	0.78					-
91	02 11 40.9	33 14 31	5	36	5	0.47					extended 2' pa 210
92	11 41.86	31 47 51.3	1.8	19	3	0.84	8.8	1.6	0.27	0.63	-
93	11 43.5	31 6 37	3	53	4	0.64					sl extended pa 340
94	11 46.50	31 59 36.1	1.8	(7)			6.9	1.2	0.34	0.01	faint red object; extended?
95	11 48.9	29 36 36	3	337	*	0.09					18m object 10"f; B2 0211+29
96	02 11 52.34	32 9 44.1	e	23	3	0.86	6.9	1.2	0.34	0.98	2nd component 2' Np; r=1.03
97	11 59.4	32 32 58	3	36	3	0.79					conf by sidelobe
98	12 1.3	31 13 59	e	87	5	0.71					14m Sb-c galaxy MCG 5-6-17 within extent; extended in pa 160 and 270
99	12 1.36	31 46 6.5	1.6	22	3	0.87	8.0	1.3	0.34	0.81	faint red object 10"Sp; sl extended pa 45, r=1.51
100	12 1.4	33 13 58	4	42	5	0.49					extended pa 150, 290
101	02 12 2.1	30 55 43	3	57	5	0.58					18m star 15"N
102	12 3.7	33 5 53	4	34	4	0.56					-
103	12 6.8	29 41 13	8	93	31	0.11					-
104	12 11.6	30 5 9	5	72	13	0.23					-
105	12 15.1	30 28 30	2	122	11	0.38					several red objects within extent extended 2' pa 150
106	02 12 17.4	31 17 54	4	27	3	0.76					3 18m stars? 10"Sp
107	12 17.5	33 32 18	7	31	7	0.35					15m SB galaxy MCG 6-6-1
108	12 21.64	32 10 16.4	1.6	(7)			5.3	0.8	0.49	0.22	r=1.09, obscured by sidelobe at 408
109	12 23.14	32 15 12.9	0.4	109	4	0.89	42.0	3.1	0.43	0.77	r=1.03
110	12 23.42	31 38 47.8	0.7	29	3	0.87	20.5	2.2	0.32	0.27	r=0.98
111	02 12 24.6	31 3 48	7	18	3	0.66					-
112	12 24.9	31 8 34	4	30	3	0.70					19m blue object 10"S
113	12 30.49	32 7 55.7	2.5	(7)			3.0	0.6	0.57	0.68	two 18m galaxies 10"Np and 15"Nf
114	12 30.8	34 5 50	2	328	71	0.14					-
115	12 35.15	32 17 49.1	2.5	15	2	0.89	3.9	0.8	0.44	1.10	confused at 408
116	02 12 37.54	32 10 10.1	e	27	2	0.91	10.4	0.8	0.59	0.78	2 components at 1407, r=1.65 See map
117	12 41.2	31 23 52	7	13	3	0.81					two 20m objects
118	12 41.54	32 22 58.8	0.7	36	3	0.88	18.7	1.8	0.36	0.52	19m red diffuse object; r=0.86
119	12 44.9	30 39 57	5	33	5	0.49					-
120	12 45.0	30 11 0	3	116	15	0.28					-

[1]	[2]	[3]	[4]	[5]	[6]	[7]	[8]	[9]	[10]	[11]	[12]
121	02 12 45.68	32 20 13.0	2.5	(7)			3.9	0.9	0.43	0.47	-
122	12 49.8	33 35 21	3	82	9	0.34					-
123	12 51.89	31 35 26.5	2.1	19	2	0.88	5.7	1.1	0.35	0.97	several faint red objects
124	12 54.2	30 49 38	e	209	12	0.57					B2 0212+30 extended: component 3' N
125	12 54.43	32 34 4.5	1.6	25	3	0.83	15.0	3.2	0.18	0.43	20m object 10"f; conf by 1407 ring; r=*
126	02 12 56.95	31 49 8.2	2.2	(<6.5)			2.8	0.5	0.67	<0.48	19m blue object 10"N
127	12 58.70	32 6 25.0	1.6	12	2	0.94	3.6	0.5	0.76	1.00	conf by grating ring at 1407; r=*
128	13 3.6	33 57 43	4	119	21	0.19					20m red object
129	13 4.81	31 34 31.0	0.9	23	2	0.89	13.7	1.5	0.37	0.42	18m blue object 15"N, three 19m galaxies 30"Sp; r=1.05, extended in pa 225
130	13 5.7	33 22 33	5	35	5	0.45					18m object 10"Np; extended 3' pa 0
131	02 13 9.60	32 11 39.8	2.7	(<6.5)			2.1	0.5	0.73	<0.91	18m object 20"S
132	13 12.3	30 13 3	6	42	8	0.30					-
133	13 14.4	33 39 39	3	97	11	0.32					-
134	13 14.93	32 25 10.1	1.0	27	3	0.90	11.2	1.2	0.41	0.70	14m Sb-c galaxy IC 1784 = MCG 5-6-19 (companion IC 1785 not detected) extended at 1407: r=2.74
135	13 20.1	31 24 45	3	36	3	0.85					S14 = 9 mJy
136	02 13 26.51	31 46 3.6	1.6	(9)			3.6	0.5	0.73	0.74	15m Sa-b galaxy MCG 5-6-22; confused r=1.76
137	13 30.00	31 54 22.1	2.4	see 139			2.0	0.4	0.90		-
138	13 30.7	30 42 20	2	76	6	0.52					19m red object 5"S, 20m red object 10"Np; extended; no pa
139	13 31.23	31 56 39.6	1.5	(6)			3.1	0.4	0.93	0.13	19m red object 10"Sf; extended; r=1.19 (137+139)
140	13 38.56	31 46 30.5	0.3	100	4	0.95	52.2	2.1	0.77	0.53	r=0.99
141	02 13 38.92	31 35 43.0	1.3	23	2	0.91	7.4	0.9	0.46	0.90	r=1.01
142	13 43.15	32 37 3.5	0.8	82	4	0.84	31.6	5.8	0.18	0.77	20m red object; extended at 1407, r=1.77
143	13 45.4	33 21 37	5	33	5	0.47					two 20m red objects 5"p and 15"f
144	13 47.8	32 32 54	6	15	2	0.87					sl extended, assoc with 142 and 148
145	13 48.70	31 50 8.3	0.4	34	2	0.96	19.3	0.8	0.88	0.45	several 20m red objects; confused at 408, r=1.09
146	02 13 50.6	29 45 0	8	72	21	0.14					19m blue object 20"Sf, 19m object 20"N;
147	13 54.5	30 58 56	5	23	3	0.67					20m blue object 10"f
148	13 56.34	32 26 14.9	0.5	65	3	0.91	22.1	1.7	0.43	0.87	faint blue object; extended, r=1.23
149	13 57.70	31 58 29.3	1.4	12	2	0.97	3.1	0.4	0.97	1.06	r=1.02
150	13 58.5	33 39 58	4	73	9	0.32					20m red object 10"N
151	02 14 1.10	31 20 32.4	0.9	175	7	0.83	35.3	*	0.13	1.30	18m objects 5"N and 10"Np; extended in pa 180; r=1.26
152	14 3.49	32 9 4.4	0.4	67	3	0.96	21.7	0.8	0.91	0.91	20m blue object 15-20"f; r=0.99
153	14 4.62	31 42 32.1	1.3	(<6.5)			5.0	0.6	0.69	<0.21	extended; r=1.47
154	14 16.9	30 5 14	6	51	10	0.25					-
155	14 23.2	30 29 37	5	39	6	0.45					-
156	02 14 29.59	31 26 47.0	1.4	42	3	0.87	12.4	2.1	0.25	0.99	3 19m objects within 15"; 2 components 4' apart, pa 30
157	14 34.8	33 7 59	5	27	4	0.59					18-19m star 1'Nf within extent irregular structure
158	14 37.2	30 42 26	5	29	4	0.53					obscured by image of 13m star
159	14 41.0	31 9 39	1	186	8	0.75					-
160	14 44.9	33 21 14	1	544	35	0.47					19m blue object, 17-18m star 15"f; B2 0214+33

[1]	[2]	[3]	[4]	[5]	[6]	[7]	[8]	[9]	[10]	[11]	[12]
161	02 14 46.18	32 6 2.5	2.0	(6.5)			2.4	0.4	0.87	0.37	-
162	14 46.4	33 31 28	4	55	7	0.38					19m object 15"Np
163	14 46.6	30 55 39	8	17	3	0.64					20m blue object, 19m object 15"N
164	14 51.0	32 53 21	e	46	3	0.72					extended 1'.5 pa 340
165	14 52.0	29 40 58	8	84	26	0.12					18m galaxy
166	02 14 52.1	33 7 37	3	44	4	0.59					-
167	14 53.4	33 44 55	6	49	9	0.28					several 18-19m objects within 10"; extended 1' pa 30
168	14 53.9	30 52 14	4	32	4	0.61					-
169	14 53.97	32 9 56.1	1.4				4.1	0.5	0.77		15m Sa galaxy IC 1789 = MCG 5-6-24; extended; r=1.30
170	14 56.4	30 35 22	2	115	9	0.47					-
171	02 15 3.56	31 39 4.5	1.5	14	2	0.92	6.1	0.8	0.47	0.69	16-17m galaxy in group; r=0.99
172	15 3.8	32 52 2	3	43	3	0.72					18m star
173a	15 6.28	32 33 19.0	1.6	113	5	0.86	13.5	2.7	0.20		several 19m red objects; both components extended, r=*, see map
b	15 11.02	32 31 35.6	0.8				26.3	3.8	0.23		
174	15 7.04	31 48 39.5	0.6	32	2	0.94	12.7	0.8	0.67	0.75	two faint blue objects; extended; r=1.37
175	15 7.38	31 46 13.0	2.7	(9)			2.5	0.6	0.62	1.0	-
176	02 15 9.45	32 4 50.4	2.1	(<6.5)			2.6	0.5	0.76	<0.74	extended in pa 270
177	15 10.67	31 53 16.9	2.7	(<6.5)			2.1	0.5	0.73	<0.91	18m star 15-20"Sp; ? extended
178	15 12.53	31 43 42.3	1.9	(9)			4.1	0.7	0.54	0.63	? extended
179	15 18.5	31 1 38	1	122	6	0.68					-
180	15 22.3	33 19 21	2	143	10	0.48					-
181	02 15 22.73	31 48 10.6	1.4	13	2	0.93	5.1	0.7	0.58	0.74	r=0.88
182	15 22.9	31 24 29	3	40	3	0.83					extended 2' pa 220
183	15 31.0	30 1 15	6	61	13	0.22					-
184	15 32.1	32 40 33	5	19	3	0.79					19m red object 10"Nf; sl extended pa 150
185	15 32.3	30 40 40	2	106	8	0.49					-
186	02 15 32.83	31 38 9.9	1.4	36	3	0.89	8.6	1.3	0.35	1.16	extended at 1407 ?; s.i. uncertain
187	15 36.8	30 52 57	5	27	4	0.59					20m red object 10"N, 18m object 10"Sf;
188	15 37.89	32 19 51.6	2.5	15	2	0.90	4.7	1.0	0.37	0.95	-
189	15 45.30	31 35 39.6	0.4	85	4	0.87	76.0	8.7	0.26	0.09	19m blue object; r=1.08
190	15 46.2	32 51 20	5	25	3	0.70					-
191	02 15 46.7	32 41 59	3	34	3	0.77					-
192	15 53.56	31 49 44.7	1.1	19	2	0.91	9.6	1.1	0.43	0.54	18m star; sl extended; r=1.10
193	15 53.1	31 25 53	6	18	3	0.81					-
194	16 1.4	34 13 59	5	164	53	0.10					14m E(?) galaxy IC 1792 = MCG 6-6-15
195	16 2.0	32 22 25	7	14	2	0.86					19-20m object 15"Np; S14 = 6 mJy
196	02 16 2.6	29 39 52	6	122	39	0.11					18m star 10"Nf
197	16 3.52	31 59 16.2	1.3	22	2	0.91	7.4	1.0	0.43	0.87	r=0.91
198	16 5.85	31 46 2.7	0.6	79	4	0.88	26.3	2.6	0.33	0.89	extended; r=1.21
199	16 12.9	33 18 5	1	243	17	0.46					B2 0216+33A
200	16 13.84	32 1 40.0	1.1	21	2	0.89	10.8	1.3	0.37	0.56	18m red object 10"S; sl extended; r=1.45

[1]	[2]	[3]	[4]	[5]	[6]	[7]	[8]	[9]	[10]	[11]	[12]
201	02 16 15.8	34 5 53	e	791	177	0.13					B2 0216+34, extended 1' pa 90
202	16 16.1	32 56 57	4	29	4	0.63					-
203	16 17.0	30 51 17	4	36	4	0.55					-
204	16 17.4	32 37 46	2	53	3	0.76					19m object 15"Np
205	16 18.0	31 51 44	2	40	3	0.88					identification difficult owing to extent; 2 components 3' apart pa 60
206	02 16 23.0	31 11 39	1	216	10	0.70					B2 0216+31
207	16 23.5	30 32 30	7	29	6	0.40					2 faint objects, 18m star 20"S
208a	16 26.71	32 31 54.7	0.3	171	7	0.78	+				several 18-19m objects; 2 components at
b	16 30.30	32 33 42.5	0.3								1407, both extended
209	16 26.9	33 22 43	4	49	6	0.41					several objects; extended irregular structure 4' pa 150
210	16 29.1	31 15 9	6	20	3	0.71					conf by sidelobe of 206
211	02 16 31.4	33 14 59	3	73	6	0.47					19m blue object, 19m blue object 15"Sf; GC 0216+33A
212	16 35.4	31 36 16	7	13	3	0.81					-
213	16 36.9	31 21 21	2	64	4	0.74					19m blue object
214	16 38.3	34 9 23	2	497	136	0.11					-
215	16 38.9	31 7 46	3	52	4	0.65					sl extended pa 180
216	02 16 40.7	31 14 33	3	49	4	0.70					several 18-19m red objects
217	16 49.8	33 34 30	1	1128	109	0.31					B2 0216+33B
218	16 53.1	32 21 19	8	13	3	0.79					19m red object in group; conf by 237
219	16 58.6	30 40 39	5	39	6	0.43					-
220	16 60.0	32 28 25	2	79	4	0.76					19m red object 10"p
221	02 17 12.6	30 58 37	2	86	6	0.55					19m blue object 10"p
222	17 12.8	31 9 41	2	95	6	0.62					extended 1'.5 pa 220
223	17 13.1	31 25 14	5	24	3	0.71					several faint objects
224	17 14.1	31 56 53	2	59	3	0.80					extended ? pa 150
225	17 16.6	32 32 34	2	60	4	0.71					-
226	02 17 17.3	32 4 33	e	13	3	0.79					20m red object; extended pa 330, conf
227	17 19.2	31 31 19	4	33	3	0.73					19m red object, 18m galaxy? 15"N
228	17 27.4	31 57 0	3	38	3	0.78					18m star 10"Sp
229	17 33.1	33 38 32	6	51	10	0.25					-
230	17 35.5	32 36 2	8	16	3	0.66					conf by sidelobe of 237
231	02 17 36.3	30 43 31	3	66	7	0.42					20m blue object 10"f; extended 40" pa 270
232	17 38.2	30 55 25	3	58	6	0.49					- (there is a 17m very blue star 3'Np between 221 and 232)
233	17 39.0	29 38 39	2	597	*	0.08					B2 0217+29
234	17 42.6	31 8 45	4	39	4	0.57					19-20m red object 10"S in group
235	17 42.6	33 6 31	5	34	5	0.46					-
236	02 17 47.3	32 43 22	3	49	4	0.60					19m red object 5"p
237	17 50.0	32 27 27	1	1402	62	0.68					19m blue star; B2 0217+32
238a	17 53.3	32 14 17	4	26	3	0.71					identification difficult; 2 components
b	18 2.5	32 12 29	4	34	3	0.70					perhaps associated, conf
239	18 11.1	30 12 19	2	211	32	0.21					B2 0218+30; component 2' away in pa 45
240	18 13.3	33 28 30	5	53	9	0.28					-

[1]	[2]	[3]	[4]	[5]	[6]	[7]	[8]	[9]	[10]	[11]	[12]
241	02 18 17.1	33 19 36	8	31	7	0.33					-
242	18 17.7	31 3 24	1	262	17	0.49					B2 0218+31
243	18 21.2	33 14 30	3	66	8	0.36					20m object
244	18 27.9	32 37 29	2	81	6	0.56					-
245	18 33.3	29 58 54	3	198	47	0.13					B2 0218+29
246	02 18 35.7	32 19 3	e	19	4	0.62					14m Sa-b galaxy IC 1793 = MCG 5-6-27; conf by sidelobe
247	18 38.1	31 46 29	2	82	5	0.63					extended pa 270
248	18 40.5	33 42 51	3	172	31	0.18					-
249	18 40.6	31 33 7	2	110	7	0.59					-
250	18 45.5	30 38 39	7	37	8	0.31					several objects within 20"; sl extended
251	02 18 50.3	34 2 40	3	358	*	0.09					19m blue object 5"f
252	18 53.9	31 49 39	4	31	4	0.60					19m objects 5"N and 15"Nf
253	18 55.5	32 18 23	3	43	4	0.58					several 20m red objects
254	18 57.6	33 53 40	5	130	36	0.12					-
255	19 7.3	30 38 2	1	271	30	0.28					19-20m blue object 10"Np; B2 0219+30A
256	02 19 7.3	33 23 15	4	86	13	0.26					20m blue object 5"p
257	19 7.6	32 27 13	7	22	4	0.53					extended 1' pa 90
258	19 17.3	33 39 48	1	450	80	0.17					19m star 10"N; B2 0219+33A
259	19 20.4	32 17 22	3	58	5	0.53					19-20m red object 15"S
260	19 29.9	30 35 11	3	119	17	0.25					-
261	02 19 35.9	30 20 37	2	244	42	0.18					B2 0219+30B
262	19 38.4	34 15 52	8	220	*	0.05					18m star 15"Sp, 20m object 15"Np
263	19 39.1	32 8 20	2	121	8	0.50					17m star 15"Sf
264	19 49.2	33 43 40	1	509	140	0.13					18m star 10"f; B2 0219+33B
265	19 57.0	32 32 2	2	132	11	0.42					19m red object
266	02 20 0.9	32 16 57	2	136	10	0.45					-
267	20 7.2	30 8 50	3	286	78	0.11					20m object; B2 0220+30
268	20 8.8	31 24 20	2	95	9	0.39					-
269	20 9.8	32 38 7	e	211	18	0.38					B2 0220+32; extended 2' pa 45
270	20 12.9	31 37 52	3	57	6	0.42					-
271	02 20 13.2	31 51 9	5	38	5	0.44					17m star 10"p, 20m object 20"Sf
272	20 19.2	32 15 57	3	81	8	0.42					-
273	20 20.5	31 7 10	3	85	10	0.32					-
274	20 23.8	31 58 15	2	101	9	0.42					15m compact galaxy MCG 5-6-36 (companion 5-6-35 not detected)
275	20 34.7	33 11 3	3	152	23	0.22					two 20m red objects
276	02 20 36.4	31 21 38	3	99	11	0.34					-
277	20 44.7	31 5 8	3	109	14	0.27					19-20m red object 15"f; component 4' S
278	20 46.9	31 16 41	8	34	8	0.31					extended?; confused
279	20 48.3	34 1 36	4	402	*	0.05					20m object; B2 0220+34, conf by ring
280	20 54.9	31 30 3	3	90	10	0.33					-

[1]	[2]	[3]	[4]	[5]	[6]	[7]	[8]	[9]	[10]	[11]	[12]
281	02 21 12.0	33 25 45	4	153	39	0.13					conf by grating ring
282	21 41.1	34 6 10	6	413	*	0.03					19m object 10"N
283	22 1.3	32 0 46	5	73	12	0.25					19m blue object
284	22 3.5	31 13 17	8	52	14	0.19					-
285	22 4.3	31 40 18	7	51	11	0.23					confused by 286; ? extended
286	02 22 9.3	31 45 54	1	372	49	0.23					19m blue star; B2 0222+31A; extended 40" pa 90
287	22 20.3	31 39 6	1	626	90	0.21					19m blue star; B2 0222+31B
288	22 19.6	31 5 28	1	883	168	0.16					B2 0222+31C
289	22 42.0	32 33 50	7	66	18	0.16					-
290	22 55.6	31 35 8	5	105	24	0.16					conf by grating ring
291	02 23 9.9	34 8 6	2	5338	*	0.01					18m star 15-20"Np; 4C 34.07, B2 0223+34
292	23 56.0	33 51 20	6	775	*	0.02					19m object 10"p; B2 0223+33, conf by grating ring

TABLE 3 The 5C7 Survey

[1]		[2]	[3]	[4]	[5]	[6]	[7]	[8]	[9]	[10]	[11]	[12]
1	08	6 36.8	27 34 16	4	477	*	0.04					B2 0806+27
2		6 44.0	28 38 11	5	1292	*	0.01					B2 0806+28
3		6 58.1	26 12 8	4	532	*	0.04					several faint objects; B2 0807+26A
4		7 6.6	27 4 31	5	250	*	0.06					-
5		7 10.1	27 50 37	4	488	*	0.05					-
6	08	7 11.2	27 40 28	1	1612	*	0.05					18m blue star 15"Np (Fanti et al 1975) B2 0807+27, 4C 27.18, MW 0806+27
7		7 23.3	26 59 44	2	574	*	0.08					B2 0807+26B
8		7 59.7	28 22 50	2	1092	*	0.04					20m blue object 5"S; B2 0807+28, MW 0807+28, conf by ring
9		8 19.3	24 58 18	6	516	*	0.02					18m galaxy 10"S (Grueff & Vigotti 1973) B2 0808+24
10		8 24.8	26 27 16	1	589	142	0.12					several 19-20m objects within 15"; B2 0808+26A
11	08	8 53.9	26 8 48	3	199	48	0.13					20m red object; Part of B2 0808+26B
12		8 56.1	26 2 46	4	156	41	0.12					Part of B2 0808+26B
13		9 4.6	27 47 0	5	126	30	0.14					-
14		9 15.5	28 5 11	e	282	74	0.12					19m galaxy 10"N; extended 30" in pa 27
15		9 17.3	26 39 13	1	533	80	0.20					19m blue object 10"N; B2 0809+26, slightly conf by grating ring
16	08	9 53.5	27 7 27	4	76	12	0.26					-
17		9 56.4	27 0 45	1	304	34	0.27					B2 0809+27
18		10 2.5	25 51 3	3	190	36	0.17					20m blue object, 17m galaxy 15"S, 19m blue object 10"N; sl conf by ring
19		10 12.2	28 11 55	3	192	39	0.16					20m red object 5"N
20		10 14.4	26 26 5	6	54	10	0.27					20m red object
21	08	10 23.2	25 7 37	e	374	*	0.08					B2 0810+25, extended 45" in pa 25
22		10 32.8	27 17 30	2	202	20	0.32					18m star 10"Sf
23		10 33.0	29 25 32	6	763	*	0.02					19m object 15"Sp; B2 0810+29
24		10 41.4	27 4 15	2	194	18	0.35					19m red object
25		10 42.7	28 0 41	1	440	58	0.23					19m red object 15"p; B2 0810+28
26	08	10 44.7	26 46 16	2	123	12	0.35					-
27		10 47.5	27 22 12	4	54	8	0.34					extended in pa 0, conf by 31
28		10 52.8	27 36 11	6	44	8	0.32					several 19m objects within 15"
29		10 54.4	26 16 44	2	132	14	0.31					18m object 15"p, 20m object 10"f
30		10 55.4	26 40 19	6	40	7	0.36					19m object 15"Nf
31	08	10 57.0	27 23 7	3	91	10	0.36					-
32		10 59.5	26 55 28	e	163	14	0.39					19m object 10"p, 20m blue object 10"N extended 2' in pa 40
33		11 13.3	26 51 0	e	110	10	0.41					19m galaxy 50"f perhaps related extended 1' in pa 90
34		11 30.0	27 32 7	4	47	6	0.40					19m red object
35		11 31.7	26 42 45	3	262	65	0.12					19m star
36	08	11 33.8	28 30 27	6	83	19	0.18					several faint objects
37		11 36.4	26 36 19	4	47	6	0.44					-
38		11 41.9	28 43 26	7	96	28	0.13					several faint objects
39		11 44.4	26 24 54	4	51	6	0.42					several faint objects
40		11 49.0	28 38 51	2	352	70	0.15					19m red object 10"f; B2 0811+28

[1]	[2]	[3]	[4]	[5]	[6]	[7]	[8]	[9]	[10]	[11]	[12]
41	08 11 54.8	28 19 10	5	66	12	0.25					20m object
42	11 57.8	25 12 53	5	114	26	0.16					20m red object
43	12 6.9	27 59 11	2	143	13	0.36					20m object, 17m star 10"Nf, 18-19m star 10"Sp
44	12 8.6	27 12 47	e	178	11	0.52					extended 1' in pa 110
45	12 14.4	26 19 18	3	58	6	0.46					19m red star
46	08 12 26.0	26 48 56	2	103	7	0.57					-
47	12 38.5	24 56 5	3	232	61	0.12					18m star 20"S; B2 0812+24
48	12 39.4	27 44 2	1	209	14	0.49					B2 0812+27
49	12 45.0	27 40 35	e	41	5	0.51					20m object 15"N; conf by 48
50	12 46.6	24 59 5	7	90	25	0.13					several faint red objects
51	08 12 53.0	28 28 3	2	147	19	0.26					19m blue star
52	13 0.1	25 46 3	6	39	6	0.37					two 18-19m red objects
53	13 3.8	26 9 23	4	39	5	0.50					20m object
54	13 26.4	26 50 44	7	17	3	0.70					-
55	13 27.0	26 56 38	e	41	3	0.70					19m star; extended 1'.5 pa 270
56	08 13 27.2	28 28 53	1	276	29	0.29					-
57	13 29.2	28 6 57	e	315	22	0.43					19m blue star, 19m red object 15"f; B2 0813+28, extended 30" in pa 140
58	13 30.3	26 26 55	2	79	5	0.64					-
59	13 32.2	29 4 40	4	212	63	0.11					-
60	13 37.2	26 43 44	5	22	3	0.71					-
61	08 13 40.8	25 26 25	4	70	10	0.31					-
62	13 44.6	25 45 47	3	61	7	0.43					several 20m objects
63	13 46.2	27 23 34	4	30	3	0.70					Extension in pa 340
64	13 47.7	25 54 9	3	72	6	0.48					19m star; slightly extended in pa 320
65	13 47.9	26 31 42	3	107	13	0.29					20m red object
66	08 13 52.6	28 58 35	4	146	34	0.14					-
67	13 54.3	26 47 35	6	19	3	0.75					18m star 10"p
68	13 57.5	26 40 47	2	66	4	0.74					-
69	13 59.5	27 29 20	6	18	3	0.71					conf by sidelobe of 85
70	14 0.7	29 27 24	2	1440	*	0.05					(18-19m star 20"N); B2 0814+29A, 4C 29.28a
71	08 14 7.4	26 5 58	5	26	4	0.59					-
72	14 8.2	25 3 57	4	93	17	0.20					20m object 5"p
73	14 16.7	28 1 44	5	28	4	0.53					19m object 15"p
74	14 17.98	27 3 52.2	1.9	43	3	0.80	13.0	3.0	0.17	0.97	20m red object; r=1.27, not resolved
75	14 30.39	27 40 10.0	0.3	198	9	0.70	+				18m star 5"Np; r=1.23, resolved
76	08 14 32.3	26 12 21	2	62	4	0.66					-
77	14 34.16	26 29 10.8	0.3	160	7	0.76	+				r=1.11, not resolved
78	14 35.1	29 14 22	1	1411	*	0.09					B2 0814+29B, 4C 29.28b, MW 0814+29
79	14 35.1	25 7 44	5	71	12	0.24					20m red object; conf by 81, perhaps extended
80	14 36.79	26 44 3.9	0.8	109	5	0.82	28.3	4.9	0.19	1.09	20m red object 10"f; r=1.37, resolved

[1]	[2]	[3]	[4]	[5]	[6]	[7]	[8]	[9]	[10]	[11]	[12]
81	0R 14 41.7	25 11 8	4	85	13	0.26					20m object 20"f
82	14 41.8	29 31 13	4	401	*	0.05					19m star 5"Sf; B2 0814+29C
83	14 43.0	25 30 17	e	28	5	0.44					ext, unreliable
84	14 45.04	26 38 56.8	1.4	70	4	0.81	18.0	3.7	0.17	1.10	several 20m objects; r=1.23, extended
85	14 45.65	27 26 1.9	0.3	700	27	0.79	305.7	*	0.12	0.67	B2 0814+27, r=1.21, prob resolved
86	0R 14 46.45	26 57 11.5	1.9	18	3	0.85	7.2	1.4	0.31	0.73	r=1.04, not resolved
87	15 4.3	24 58 30	2	297	45	0.20					19m blue object 20"f; B2 0815+24
88	15 4.02	26 45 37.2	1.0	51	3	0.86	13.7	1.7	0.32	1.05	r=0.92, not resolved
89	15 5.2	27 29 41	3	41	3	0.81					conf by sidelobe of 85
90	15 8.9	26 14 18	5	21	3	0.72					several 19-20m objects 15"Nf; confused
91a	0R 15 9.63	26 52 7.8	1.2	(<10)			8.9	1.1	0.41	<0.09	several red objects in field; r=0.59
b	15 16.04	26 52 34.6	2.5				3.7	0.8	0.45		r=*, perhaps associated with 94
92	15 12.5	28 18 34	e	109	8	0.46					extended 50" in pa 40
93	15 16.6	28 36 5	e	47	8	0.32					ext, unreliable
94	15 17.26	26 54 59.2	1.3	22	2	0.90	6.9	0.9	0.48	0.94	several 18-19m objects; r=0.85, probably ext; conf at 408
95	15 19.1	24 44 53	e	234	52	0.14					19-20m blue object 20"N; ext 30" pa 200
96	0R 15 23.5	25 5 19	5	65	12	0.25					20m object
97	15 23.8	28 22 58	5	42	6	0.43					-
98	15 24.0	28 17 44	5	34	5	0.47					-
99	15 24.6	27 30 22	6	15	3	0.83					conf by sidelobes
100	15 25.8	25 28 6	2	144	12	0.39					-
101	0R 15 31.71	26 25 43.0	2.1	43	3	0.81	15.5	*	0.13	0.83	r=*; perhaps extended in pa 320 at 408
102a	15 35.73	27 18 29.4	2.5				4.1	0.9	0.41		16m E? galaxy MCG 5-20-8; r=*, extended
b	15 41.86	27 17 48.7	0.7	30	3	0.90	15.3	1.3	0.45		r=1.34, resolved
103	15 41.74	26 40 23.1	1.8	(<10)			5.8	1.0	0.41	<0.44	18m galaxy; r=*
104	15 49.2	25 28 20	5	37	6	0.41					ext, unreliable
105	15 50.40	27 15 18.0	2.0	16	2	0.91	3.8	0.7	0.55		r=1.38, conf at 408, perhaps associated with 107
106	0R 15 50.96	26 33 18.9	0.3	616	21	0.87	189.3	18.6	0.31	0.95	two 19m red objects; B2 0815+26,r=1.26, resolved in pa 90
107a	15 56.93	27 18 24.2	0.6	48	3	0.91	15.5	1.1	0.51	0.91	19m star 10"N, 20m object 10"Nf; r=1.10,
b	15 58.55	27 17 9.3	2.4				3.3	0.7	0.55		resolved in pa 140, see map
108	15 58.10	27 34 22.1	2.4				9.6	2.5	0.18		19m star 5"f; r=*
109	15 58.36	27 5 21.1	2.6				2.1	0.5	0.75		19m object 10"p; r=*
110	16 5.80	27 26 59.9	1.6	(12)			8.1	1.2	0.34	0.37	18m blue star 10"N; r=1.06, not resolved
111	0R 16 7.41	26 24 11.1	0.3	913	33	0.84	268.8	47.5	0.17	0.99	20m blue object (Grueff & Vigotti 1973) B2 0816+26A, r=0.96, not resolved
112	16 10.08	27 2 44.4	1.1	(<10)			4.7	0.4	0.84	<0.61	19m blue star; r=1.13, not resolved
113	16 12.2	28 2 3	3	43	4	0.64					19m object 10"Nf; conf by sidelobe of 119, perhaps extended
114	16 12.3	29 3 21	6	79	19	0.17					-
115	16 12.7	28 47 31	5	63	11	0.26					-
116	0R 16 14.1	25 55 34	2	76	5	0.64					19m blue object 15"S, several 19m objects 15"f
117a	16 14.73	27 17 1.3	1.1	27	2	0.93	6.7	0.7	0.62		two 19m objects near (a); r=0.88 for 2
b	16 15.87	27 15 28.6	2.2				2.9	0.5	0.66		components, uncertain
118	16 15.03	26 51 28.5	0.3	661	21	0.94	205.9	7.8	0.80	0.94	19m UV-excess object (Fanti et al 1975) B2 0816+26B, sl extended at 140?
119	16 15.8	27 56 56	1	239	11	0.69					19m blue star
120	16 17.5	25 17 4	3	100	11	0.34					20m blue object

[1]	[2]	[3]	[4]	[5]	[6]	[7]	[8]	[9]	[10]	[11]	[12]
121	08 16 19.07	27 4 59.7	0.5	35	2	0.95	13.1	0.6	0.87	0.79	r=0.98, not resolved
122	16 26.88	26 41 21.2	0.4	90	4	0.93	28.0	1.5	0.60	0.94	r=1.06, not resolved
123	16 27.0	25 8 8	3	86	12	0.28					-
124	16 27.4	27 46 17	4	28	3	0.77					-
125	16 27.6	25 28 48	1	436	31	0.43					B2 0816+25
126	08 16 38.1	25 31 49	1	166	12	0.45					slightly extended ?
127	16 40.68	27 19 27.9	0.9	26	2	0.93	8.3	0.7	0.62	0.93	r=1.28, resolved; at 1407 MHz faint extensions to N & S embrace 130
128	16 42.04	26 51 18.2	2.3				2.1	0.4	0.89		3 19m objects; r=*
129	16 42.75	27 14 49.6	2.4				2.3	0.5	0.76		18m star 10"N; r=*
130	16 43.81	27 11 22.7	1.1	(<11)			4.6	0.4	0.85	<0.72	18m star 20"Sf; r=1.02, not resolved
131	08 16 46.3	28 23 28	5	39	5	0.46					-
132	16 47.0	28 46 50	2	213	25	0.27					19m object 10"N
133a	16 50.74	26 53 42.0	0.8	13	2	0.96	6.0	0.4	0.94		19m star between (a) and (b); r=1.10, extended pa 90, conf at 408
b	17 0.04	26 53 30.8	2.6				1.7	0.4	0.94		r=*
134	16 53.9	25 43 0	2	107	7	0.54					-
135	16 58.23	26 58 36.5	0.8	14	2	0.97	6.0	0.4	0.97	0.68	20m object; r=1.34, resolved; conf at 408
136a	08 17 0.9	26 19 33	3	29	3	0.83					19m red object and 20m blue object between (a) and (b)
b	17 2.5	26 18 26	5	22	3	0.82					
137	17 1.5	25 46 44	1	127	8	0.58					-
138	17 2.7	24 21 38	6	185	*	0.07					20m object 20"S
139	17 4.50	26 34 31.7	1.2	16	2	0.92	8.1	0.9	0.45	0.55	r=1.06, not resolved
140	17 10.04	27 28 2.0	1.6	17	2	0.89	7.0	1.1	0.39	0.72	20m red object; r=*, conf at 408
141	08 17 8.36	27 36 0.9	1.1	112	5	0.85	19.5	3.3	0.21	1.41	r=1.08, not resolved
142	17 16.55	26 22 32.2	0.8	102	4	0.85	31.5	5.7	0.18	0.95	two 20m red objects; r=1.27, extended pa 170, see map
143	17 17.6	27 33 47	6	16	2	0.87					20m red object
144	17 18.5	25 29 21	2	112	9	0.43					several faint red objects
145	17 20.8	27 52 46	1	349	15	0.73					20m red objects; B2 0817+27
146	08 17 20.7	29 4 25	3	195	38	0.16					-
147	17 24.40	27 6 19.0	1.1	(<10)			4.2	0.4	0.93	<0.70	two 19m red objects; r=1.49, extended pa 250
148	17 24.5	24 28 6	5	197	*	0.09					-
149a	17 26.75	27 30 46.8	e	94	4	0.88	11.6	1.6	0.31		20m object 10"N from (a), 18m object
b	17 29.72	27 29 28.9	e				13.1	1.6	0.34		20"S from (b); see map
150	17 28.1	25 56 55	e	22	3	0.66					extended
151	08 17 30.2	28 3 27	5	26	4	0.64					-
152	17 37.9	27 44 0	7	15	3	0.79					-
153	17 43.16	27 2 18.8	0.4	58	3	0.96	18.8	0.7	0.90	0.91	r=1.18, resolved
154	17 44.27	26 55 4.4	1.6	(<10)			3.0	0.4	0.87	<0.97	18m object 15"Np; r=1.38, resolved
155	17 49.5	25 39 37	2	117	8	0.51					-
156	08 17 49.6	28 43 54	4	65	10	0.29					-
157	17 49.74	27 16 29.3	1.6	(<10)			4.1	0.6	0.63	<0.72	r=0.94, not resolved
158	17 50.83	27 4 23.0	1.8	(<10)			2.8	0.4	0.85	<1.03	19m red object; r=*, slightly extended in pa 270
159a	17 55.69	26 [illegible] 11.8	0.9	13	2	0.95	5.9	0.5	0.79		18m star 15"Sp from (a); r=0.99
b	18 2.52	26 53 57.4	2.5				2.3	0.5	0.77		r=*
160	17 57.87	26 27 55.7	2.6	17	2	0.87	6.8	1.7	0.24	0.72	r=*

[1]	[2]	[3]	[4]	[5]	[6]	[7]	[8]	[9]	[10]	[11]	[12]
161	08 17 59.62	27 10 21.3	1.6	(10.6)			3.8	0.5	0.72	0.83	17m star, 18m star 15"S; r=1.32, not resolved
162	18 8.22	27 18 3.5	0.8	41	3	0.92	11.0	0.9	0.51	1.07	19m star 15"S; r=1.05, not resolved
163	18 8.6	28 42 22	5	54	9	0.30					-
164	18 8.7	27 43 22	6	17	3	0.78					19-20m red object
165	18 8.8	26 41 54	6	14	2	0.92					-
166	08 18 9.5	25 39 22	2	105	8	0.50					17m star 15"f
167a	18 11.22	27 26 54.9	1.9	16	2	0.88	7.0	1.3	0.31		two 19m objects near (b); r=1.26, not
b	18 13.72	27 29 2.6	5.2	18	2	0.87					resolved, low-brightness halo
168	18 12.87	26 58 49.6	0.9	22	2	0.95	6.5	0.5	0.73	0.98	r=*, 2 components at 1407
169	18 17.4	28 37 27	6	43	7	0.33					19m object 10"S, 19m red object 15"Sp extended in pa 90
170	18 21.5	25 28 38	1	386	28	0.41					group of 20m objects within 15"; B2 0818+25
171	08 18 23.6	28 49 29	3	104	15	0.25					-
172	18 25.31	26 34 59.0	1.2	(12)			11.5	1.6	0.31	0.03	r=0.99, not resolved
173	18 25.6	28 14 24	e	49	5	0.52					extended 2' S
174	18 27.23	27 22 51.4	e	74	3	0.89	33.1	3.1	0.34	0.65	19m very red object 15"Np; r=1.45, extended 30" in pa 45
175	18 33.81	27 27 40.4	0.5	40	3	0.86	40.5	5.4	0.23	-0.01	r=1.31, resolved
176	08 18 43.1	26 53 57	7	13	2	0.92					-
177	18 43.56	27 34 2.1	0.3	24	3	0.82	+				r=*, conf at 408 by 180, perhaps extended
178	18 44.3	29 32 2	3	585	*	0.05					18m blue star 20"p, 20m red object 5"f B2 0818+29
179	18 48.3	27 39 4	2	58	3	0.78					extended pa 250
180	18 50.07	27 31 10.5	2.0	63	3	0.83	16.3	*	0.13	1.09	19m star 15"Np; r=1.02, not resolved, conf at 408
181	08 18 49.9	29 7 19	5	134	34	0.13					18m blue object
182	18 52.2	26 31 15	4	25	3	0.84					-
183	18 53.8	25 25 32	6	34	6	0.38					20m red object 20"N
184	18 56.6	28 46 38	4	78	12	0.25					17m star 20"f
185	18 57.8	28 37 48	2	187	19	0.31					slightly extended in pa 270
186	08 18 58.71	26 40 2.5	1.1	19	3	0.87	14.5	2.1	0.26	0.21	r=1.13, not resolved
187	19 0.41	26 45 40.6	2.5				5.3	1.2	0.32		18-19m star; r=*
188	19 0.9	28 5 25	e	46	4	0.57					extended 2-3' in pa 150
189	19 1.1	27 37 55	1	95	5	0.78					18-19m blue star; perhaps associated with 179
190	19 2.74	27 6 31.5	0.5	36	3	0.89	31.1	2.6	0.38	0.12	20m blue object; r=1.12, resolved: low-brightness halo
191	08 19 5.3	27 44 40	6	18	3	0.73					19m object 10"Sp
192	19 6.56	26 53 55.8	2.0	15	2	0.89	5.8	1.1	0.36	0.77	r=*
193	19 13.0	27 [illegible] 33	5	22	3	0.75					-
194	19 14.3	25 48 10	1	752	43	0.53					18m blue star; B2 0819+25
195	19 19.9	28 15 37	1	438	28	0.47					B2 0819+28
196	08 19 32.4	27 12 1	5	20	3	0.84					-
197	19 33.12	26 54 34.6	1.3	67	3	0.85	14.7	2.5	0.23	1.22	18m and 19m objects; r=1.07, extended in pa 220 at 1407, pa 150 at 408
198	19 33.7	26 41 23	6	17	3	0.82					-
199	19 37.7	25 52 51	6	27	4	0.54					-
200	19 46.1	26 32 55	4	26	3	0.77					-

[1]	[2]	[3]	[4]	[5]	[6]	[7]	[8]	[9]	[10]	[11]	[12]
201	0R 19 46.7	27 41 12	4	33	3	0.70					9m star 10"Np
202	19 53.8	27 6 51	e	40	3	0.81					extended 1'.5 in pa 270
203	19 54.3	26 15 50	4	33	3	0.68					-
204	19 58.2	25 30 50	3	67	8	0.37					19-20m object 15"Np
205	20 0.1	24 40 19	1	709	209	0.10					B2 0820+24A, AO 0820+24
206	0R 20 10.2	28 1 12	4	37	5	0.52					20m blue object
207	20 13.6	27 30 33	6	21	3	0.71					-
208	20 18.6	25 6 18	1	370	53	0.21					B2 0820+25
209	20 19.4	28 24 23	e	43	7	0.35					20m object 15"f, 20m red object 15"Nf extended 2' pa 220
210	20 19.9	26 42 0	7	17	3	0.75					-
211	0R 20 23.2	25 41 10	e	35	6	0.41					19m blue object 20"N; sl ext pa 15
212	20 30.2	27 1 28	3	40	3	0.75					-
213	20 34.1	28 14 9	2	160	13	0.40					20m red object
214	20 36.4	29 38 11	4	772	*	0.03					18.5m quasar: z=2.368 (Wills & Wills 1976); B2 0820+29
215	20 37.1	25 59 6	2	71	6	0.51					-
216	0R 20 38.0	26 17 46	5	27	4	0.62					20m object 10"Sf
217	20 41.6	26 32 28	6	22	3	0.68					-
218	20 43.9	27 34 55	3	42	4	0.64					19-20m red object
219	20 44.9	28 41 47	5	74	14	0.22					-
220	20 52.3	28 16 22	6	40	7	0.37					chain of 4 17m stars(?)
221	0R 20 56.5	27 53 11	4	42	5	0.51					two 20m blue objects
222	20 58.4	24 56 27	e	102	26	0.14					extended 1'.5 in pa 40
223	21 5.8	26 37 48	1	239	12	0.65					20m object, 19m red object 20"Np; B2 0821+26
224	21 8.9	25 29 32	4	72	10	0.30					-
225	21 20.6	27 19 49	7	20	4	0.62					-
226	0R 21 21.3	26 19 13	3	62	5	0.54					19m object
227	21 23.6	26 41 20	4	30	4	0.62					two 20m red objects 20"Sf; conf by sidelobe of 223
228	21 23.6	25 8 2	6	74	17	0.18					-
229	21 29.5	25 52 33	2	178	14	0.40					extended 30" in pa 270
230	21 34.1	24 48 34	3	292	*	0.10					19m blue star; B2 0821+24
231	0R 21 37.8	25 7 42	3	188	36	0.17					-
232	21 37.9	27 23 20	4	33	4	0.57					20m red object, 19m red object 10"Sf
233	21 42.7	26 53 1	4	39	4	0.60					-
234	21 46.6	27 46 56	6	27	5	0.46					perhaps extended in pa 90
235	21 58.9	25 58 29	4	60	7	0.38					-
236	0R 22 11.4	27 19 52	2	70	6	0.51					-
237	22 12.3	26 41 27	1	207	13	0.51					0822+26W1, slightly extended
238	22 13.6	26 49 48	5	35	4	0.52					17m star 10"Sp; 0822+26W2
239	22 20.7	27 56 59	3	87	9	0.36					-
240	22 24.9	26 8 44	e	202	17	0.39					extended 1' in pa 140

[1]	[2]	[3]	[4]	[5]	[6]	[7]	[8]	[9]	[10]	[11]	[12]
241	08 22 35.4	27 10 39	e	193	13	0.47					extended in pa 40
242	22 44.1	24 50 24	6	184	*	0.07					19m object 15"f
243	22 45.8	27 14 15	e	156	11	0.45					19m blue star; 0822+27W1, extension 1'.5 in pa 90
244	22 50.5	27 42 15	6	40	7	0.37					-
245	22 55.7	26 53 50	1	685	47	0.44					18m star 15"N; B2 0822+26, 0822+26W3
246	08 22 56.3	26 58 58	6	29	5	0.44					19m object 10"Sp; conf by sidelobe of 245
247	22 59.2	26 2 51	5	48	8	0.31					extended in pa 0
248	23 4.1	27 47 34	2	110	12	0.32					18m object in group of three
249	23 7.4	26 13 3	2	119	12	0.33					-
250	23 8.8	23 13 34	3	143	22	0.22					18m galaxy, 19m star 5"Nf
251	08 23 10.3	27 2 16	4	53	6	0.41					0823+27W1
252	23 13.1	26 36 9	2	127	11	0.38					0823+26W1
253a	23 13.9	27 23 19	6	33	6	0.37					19m red object 20"p from (a)
b	23 22.0	27 24 43	4	53	7	0.36					
254	23 22.0	28 42 45	3	251	*	0.10					extended 1' in pa 0
255	23 36.6	26 50 35	3	94	10	0.35					0823+26W2
256	08 23 50.6	26 47 9	3	84	10	0.33					pulsar AP 0823+26, extended pa 270?
257	24 6.4	28 22 15	4	187	48	0.13					-
258	24 6.4	27 26 41	4	83	12	0.27					-
259	24 8.5	26 18 17	4	91	14	0.25					20m red object
260	24 18.1	26 8 36	6	59	13	0.21					empty field, curious 13m galaxy 1'p
261	08 24 21.4	29 28 44	1		*						19m galaxy; B2 0824+29, 3C200, 4C 29.29
262	24 25.2	27 20 29	5	68	12	0.25					-
263	24 29.4	28 39 7	5	243	*	0.07					19m object
264	24 32.9	26 47 9	2	175	22	0.25					19m blue object; 0824+26W2
265	24 39.2	27 10 34	5	63	12	0.24					20m red object 10"p; 0824+27W1
266	08 24 40.2	27 45 36	3	135	24	0.19					20m blue object
267	24 48.1	27 23 55	2	219	32	0.21					-
268	24 55.2	26 49 30	6	67	13	0.22					0824+26W3
269	25 39.3	25 38 33	5	250	*	0.07					-
270	25 41.8	24 46 39	2	1792	*	0.02					B2 0825+24, 4C 24.17, PKS 0825+24, extended 40" in pa 90
271	08 26 0.2	25 4 10	6	475	*	0.03					B2 0825+25